

CLASH OF MINLP RELAXATIONS: PIECEWISE LINEAR VS. GLOBAL PARABOLIC

ADRIAN GÖß 

ABSTRACT. Solving mixed-integer nonlinear programs (MINLPs) typically relies on constructing relaxations that are easier to tackle than the original problem. Recently, global parabolic (PARA) relaxations were introduced, featuring separable quadratic functions – paraboloids – as global under- or overestimators of general nonlinear constraint functions. So far, the paraboloids are all computed at once by solving a mixed-integer linear program (MIP). For small tolerances or wide function domains, the corresponding MIP grows in size and is eventually intractable, preventing a meaningful comparison with established relaxation techniques.

We therefore propose a novel iterative method to compute PARA approximations that succeeds on all tolerance-domain combinations where the original one has failed. The computational study is preceded by a thorough theoretical explanation and analysis. Finally, the improved method enables a computational comparison with piecewise linear (PWL) relaxations in terms of runtime on general MINLP instances.

The results show that the modern solver SCIP can solve PWL relaxations faster when the tolerance is high, shifting strongly in favor of PARA for tighter tolerances. We attribute the effect to the difference in the corresponding problem size: PWL relaxations introduce binary variables to identify the active linear piece and their number grows with decreasing tolerance. PARA, on the other hand, does not require additional variables such that the dimension is maintained. For problems with at least one (co)sine constraint, the effect significantly amplifies. Thereby, for medium tolerances, PARA relaxations outperform SCIP stand-alone. Applied problems like alternating current optimal power flow (AC-OPF) feature such constraint types, leaving PARA a viable relaxation strategy.

1. INTRODUCTION

The modeling power of mixed-integer nonlinear programming (MINLP) is undisputed. The combination of integral components and nonlinear interconnection allows for the resemblance of a great variety of applications. These range from gas network control [30] over chemical processes [2] up to the design of water networks [8]. Along with this power comes a certain (computational) cost, which makes it hard to solve general mixed-integer nonlinear programs (MINLPs) at scale and necessitates a retreat to simplified models, at least as an intermediate step. For instance, in modern optimization software for MINLP like BARON [37], COUENNE [6], Gurobi [27], SCIP [28], or XPRESS [22] relaxations of the original problem are constructed and then solved.

(A. Göß) UNIVERSITY OF TECHNOLOGY NUREMBERG, ANALYTICS & OPTIMIZATION, DR.-LUISE-HERZBERG-STR. 4, 90461 NUREMBERG, GERMANY

E-mail address: adrian.goess@utn.de.

Date: March 18, 2026.

2010 Mathematics Subject Classification. 90C11, 90C20, 90C26, 90C30.

Key words and phrases. Mixed-integer Nonlinear Programming, Relaxations, Mixed-Integer Linear Programming, Mixed-Integer Quadratically-Constrained Programming.

A popular technique to construct relaxations of problems with general nonlinear constraints is their piecewise handling. With the advances in mixed-integer linear programming (MIP) throughout the last decades, constructing relaxations based on linear functions appears as a potentially successful option. In fact, piecewise linear (PWL) relaxations have been originally introduced in [31] – to the best of our knowledge – and are further developed and adjusted every since, e.g., see [3, 12, 16, 29, 36]. Also refer to [41] for an extensive survey and to [9] for a recent computational comparison. As far as we are aware, all of the aforementioned solvers include such relaxations.

There also exist piecewise techniques beyond the linear realm. For instance, the SC-MINLP approach [18, 20] can be seen as an extension of PWL. For a nonlinear and twice continuously differentiable function f , it divides the function domain into intervals on which f is either convex or concave, respectively. Then, the concave parts are relaxed by PWL, whereas the convex parts remain. This renders the resulting relaxed problem a convex MINLP, which is considered (more) tractable. Even more general approaches feature piecewise quadratic [40] or piecewise polynomial approximates [17]. The resulting problems fall into the class of mixed-integer quadratically-constrained programming (MIQCP), at least after reformulation. Though MIQCP is still a subclass of MINLP, there exist tailored approaches to solve such problems [3, 4, 10, 11, 21, 33, 34, 42].

All those piecewise approaches have the benefit to construct relaxations that can fulfill a prespecified tolerance. That is, given a tolerance $\varepsilon > 0$, one can compute approximates, i.e., pieces of linear/quadratic functions, that fulfill the ε -accuracy with respect to the original problem. Thus any solution to the relaxed problem constitutes an ε -approximate solution which often suffice in practice. As an additional advantage, the character of the relaxed problem as a MIP or MIQCP problem allows to leverage tailored solvers.

Naturally, those benefits are not without cost. Depending on the modeling technique, they come with the introduction of binary variables whose number grows with the number of pieces. The approximates – e.g., linear pieces – lack a global validity, i.e., they do not constitute global under-/overestimators of the constraint function, and thus need to be “disabled” outside their corresponding interval. Hence, the resulting relaxation grows in (variable) size, which may impose computational challenges for large problems or tight tolerances. In a first attempt to circumvent additional integer variables, the authors of [26] introduced a framework to compute global parabolic (PARA) approximations of functions. The approximates are *paraboloids*, i.e., separable quadratic functions, globally under-/overestimating a constraint function. Although not necessarily being convex, the global validity allows to incorporate the paraboloids as constraints without the necessity of additional binary variables. That is, the problem size grows in the number of constraints only, but some solvers like SCIP seem to handle those similar-shaped constraints quite well, compare [26].

Although the PARA approach seems to be a viable relaxation technique, the method to compute respective PARA approximations in [26] is computationally limited. It computes all approximating paraboloids at once by repetitively solving MIP problems. Thereby, their size grows with domain width and decreasing tolerance, leaving them eventually not solvable under limited resources. Consequently, [26] reports valid parabolic approximations only on artificial domains and with respect to moderate tolerances, preventing a meaningful comparison with established techniques like PWL.

We thus introduce a novel iterative method that leverages differentiability of the constraint functions in combination with a factorable problem structure to compute

PARA approximations for tight tolerances and wide domains. In Section 3, we introduce our method formally, give proof of its correctness, and showcase that it is indeed able to succeed on tolerance-domain combinations that are left as unsolved by the approach in [26]. Furthermore, our method then allows for a comparison against PWL relaxations in terms of numbers of approximates – linear pieces versus parabolas – (Section 3.2.2) and computational efficacy (Section 4).

The remainder is dedicated to establish common ground in Section 2 by a presentation of the notation and the optimization problem. Further, it gives a short introduction into PWL (Section 2.3) and the original PARA approach (Section 2.4). We close the article with some concluding remarks in Section 5. Proofs and additional results can be found in Appendix A and Appendix B, respectively.

2. PRELIMINARIES

Before diving into the main topic of the article, we want to clarify notation and state the problem(s) in question. During later statements and proofs this will foster clarity. Additionally, we aim to explain basic concepts such as the relaxation techniques.

2.1. Notation. Consider the naturals without zero $\mathbb{N} = \{1, 2, 3, \dots\}$. We will use n' , $n \in \mathbb{N}$ as the original variable dimension and the variable dimension after reformulation, respectively, and m' , $m \in \mathbb{N}$ as the number of original constraints and constraints of interest, respectively. For counting or numbering variables, constraints, or other objects, we introduce the short notation $[n] := \{1, 2, \dots, n\}$. Vectors are given in bold such as $\mathbf{x} \in \mathbb{R}^n$, whereas components are italicized, e.g., $\mathbf{x} = (x_1, \dots, x_n)^\top$. For an interval $\mathcal{D} = [\underline{x}, \bar{x}]$, we denote its length by $|\mathcal{D}| := |\bar{x} - \underline{x}|$, using $\mathcal{D} \neq \emptyset$ and $|\mathcal{D}| > 0$ interchangeably. The interior is denoted by $\text{int}(\mathcal{D}) = (x, \bar{x})$.

2.2. Mathematical Problem. We consider general MINLP problems of the form

$$\begin{aligned} \min_{\mathbf{x}' \in \mathbb{R}^{n'}} \quad & c(\mathbf{x}') \\ \text{s.t.} \quad & g_j(\mathbf{x}') \leq 0, \quad j \in [m'], \\ & x'_i \in \mathbb{Z}, \quad i \in I, \\ & \mathbf{x}' \in [\underline{\mathbf{x}}', \bar{\mathbf{x}}'], \end{aligned} \tag{P}_{\text{gen}}$$

where $I \subseteq [n']$. The vectors $\underline{\mathbf{x}}'$ and $\bar{\mathbf{x}}'$ denote component-wise bounds to \mathbf{x}' , which we assume to be finite. Note that this kind of formulation is no restriction, i.e., it does include equality constraints by re-modeling $g(\mathbf{x}') = 0$ to $g(\mathbf{x}') \leq 0$ and $-g(\mathbf{x}') \leq 0$.

The involved functions are assumed to be sufficiently smooth, which is common in MINLP, see, e.g., [19]. That is, we assume them to be once continuously differentiable and, if necessary, to be able to compute their optimum over any compact domain. Depending on the particular method the latter can require twice continuous differentiability.

We also assume the involved functions to be *factorable*, see, e.g., [5, 32]. That is, they are composed of finitely many binary operations (sum, product, division, power) and finitely many unary operations (sin, cos, exp, log, $|\cdot|$) of constants and variables. Equivalently, factorable functions can be expressed in terms of an expression tree which has the mentioned operations as nodes as well as variables and constants as leaves. For a given non-leaf node N , the child node(s) represents the argument(s) of the operation in N . More detailed explanations can be found in [5, 14, 25, 35, 38]. Nearly all instances from MINLPLib [13] are available in the OSiL file format [23], which directly provides the expression tree structure.

The factorability allows to rewrite the original problem formulation in terms of bivariate products and one-dimensional functions by introduction of auxiliary variables in place of intermediate nodes. For example, consider $g(\mathbf{x}') = \sin(x'_1 x'_2)^2$. By introduction of variables \tilde{x} and y we can rewrite the constraint $g(\mathbf{x}') \leq 0$ to $y^2 \leq 0$, $y = \sin(\tilde{x})$, and $\tilde{x} = x'_1 x'_2$. Note that finite bounds on \mathbf{x}' can be propagated to \tilde{x} and y . For instance, $x'_1 \in [1, 2]$ and $x'_2 \in [0, \pi/4]$ result in $\tilde{x} \in [0, \pi/2]$ and $y \in [0, 1]$.

Those reformulations, as performed by the modern MINLP solvers cited in the introduction, allow us to focus on one-dimensional, general nonlinear constraint functions only. For this purpose, we denote them after reformulation as f_j , e.g., $f_1(\tilde{x}) = \sin(\tilde{x})$, and collect all linear and quadratic constraints (including bounds) as well as integrality restrictions in a set Ω . Furthermore, vector \mathbf{x} represents a concatenation of \mathbf{x}' – and newly introduced $\tilde{\mathbf{x}}$ -variables, whereas the \mathbf{y} -variables are kept for clarity. In conclusion, we assume our problem at hand to be presented as

$$\begin{aligned} \min_{(\mathbf{x}, \mathbf{y}) \in \mathbb{R}^n \times \mathbb{R}^m} \quad & c(\mathbf{x}) \\ \text{s.t.} \quad & f_j(x_{i_j}) \leq y_j, \quad j \in [m], \\ & (\mathbf{x}, \mathbf{y}) \in \Omega. \end{aligned} \tag{P}$$

The number of \mathbf{x} -variables is now denoted by n , whereas m is the number of “interesting” constraints and \mathbf{y} -variables. The subindex j of i_j indicates that a variable x_i may occur in several constraints j .

Note that the constraint functions f_j are only defined on a one-dimensional and finite domain, but remain general nonlinear ones. Therefore, despite any reformulation, it cannot be expected to compute an exact solution to (P). Instead, in practice the user specifies an approximation tolerance $\varepsilon > 0$ and is satisfied when obtaining an ε -approximate solution, i.e., a point that violates the nonlinear constraints by a value of at most ε . Such a point is equivalent to an exact optimal solution of the problem

$$\begin{aligned} \min \quad & c(\mathbf{x}) \\ \text{s.t.} \quad & f_j(x_{i_j}) \leq y_j + \varepsilon, \quad j \in [m], \\ & (\mathbf{x}, \mathbf{y}) \in \Omega. \end{aligned} \tag{P_\varepsilon}$$

For computing an ε -approximate solution, a natural idea is to substitute f_j in (P) by an ε -relaxation \hat{f}_j , i.e., it holds that $f_j - \hat{f}_j \leq \varepsilon$ on the domain of f_j . The resulting relaxed problem reads

$$\begin{aligned} \min \quad & c(\mathbf{x}) \\ \text{s.t.} \quad & \hat{f}_j(x_{i_j}) \leq y_j, \quad j \in [m], \\ & (\mathbf{x}, \mathbf{y}) \in \Omega. \end{aligned} \tag{P_{rel}}$$

A solution $(\mathbf{x}^*, \mathbf{y}^*)$ for (P_{rel}) then fulfills $f_j(x_{i_j}^*) \leq \hat{f}_j(x_{i_j}^*) + \varepsilon \leq y_j^* + \varepsilon$ for $j \in [m]$ and is thus a valid ε -approximate solution.

A strategy for computing a linear \hat{f}_j , which has regained recent attention, is the approach by piecewise linear functions. In the following, we provide an introduction of it.

2.3. Piecewise Linear Model. We consider a nonlinear function f and a finite domain $\mathcal{D} = [\underline{x}, \bar{x}]$ such that $\underline{x} < \bar{x}$. First, we will explain the computation and modeling of a piecewise linear (PWL) *approximation*, before extending it to a PWL *relaxation*. A PWL approximation \bar{f} of f can be constructed as a linear interpolation of f and is thus defined by breakpoints $\{t_0, t_1, \dots, t_K\}$ with $t_0 = \underline{x}$, $t_K = \bar{x}$, and

$t_{k-1} < t_k$ for $k \in [K]$. Parameter $K \in \mathbb{N}$ denotes the number of intervals/linear pieces. Then, for $x \in [t_{k-1}, t_k]$, it is

$$\bar{f}(x) = f(t_{k-1}) \frac{t_k - x}{t_k - t_{k-1}} + f(t_k) \frac{x - t_{k-1}}{t_k - t_{k-1}}.$$

Given an approximation tolerance $\varepsilon > 0$, we describe one way to compute \bar{f} . Starting with $K = 1$, $t_0 = \underline{x}$, $t_1 = \bar{x}$, we check the condition $|\bar{f}(x) - f(x)| \leq \varepsilon$ for all $x \in [t_0, t_1]$. Since such a check can be performed by computing the maximum/minimum of the difference, the aforementioned sufficient differentiability comes into play. If the condition is met, \bar{f} is a valid ε -approximation of f . Otherwise, we execute a binary search for the largest t_1 to fulfill the condition. After t_1 is determined, we increment K and start to find the largest t_2 such that the condition is met on $[t_1, t_2]$. The procedure is iterated and stops when $t_K = \bar{x}$. We refer to [9] for a current implementation.

Besides its computation, the more important aspect is the incorporation of a PWL approximation \bar{f} into an optimization model. To the best of our knowledge, a PWL formulation was first introduced in [31]. The method explained there is referred to as *incremental method* or *δ -method*. In the meantime, there have been established several adjusted formulations, see [3, 12, 16, 29, 36], that try to improve computational performance, e.g., by reducing the number of variables in the model. Recently though, Braun and Burlacu [9] demonstrated that in some settings the incremental method is still superior to all other methods in terms of computational performance. Therefore, we choose it for our computational comparison later on and explain it in the following, rephrasing mainly from [9].

For a given $x \in \mathcal{D}$, we first need to determine the corresponding interval index $\bar{k} \in [K]$ such that $x \in [t_{\bar{k}-1}, t_{\bar{k}}]$. In the incremental method, we introduce one binary variable u_k for each but the last interval $[t_{k-1}, t_k]$, $k \in [K-1]$, and aim to have $u_k = 1$ for all intervals with $t_k \leq x$, else $u_k = 0$. In other terms, the binary variable u_k is activated whenever x exceeds the upper bound of the corresponding k th interval until the interval containing x is reached. Formally, this can be ensured by

$$\begin{aligned} t_0 + \sum_{k=1}^{K-1} u_k (t_k - t_{k-1}) &\leq x, \\ u_{k+1} &\leq u_k, \quad \text{for } k \in [K-1]. \end{aligned}$$

Besides determining the relevant interval $[t_{\bar{k}-1}, t_{\bar{k}}]$, we second need to compute the relative distance of x inside it. Here, the incremental method advocates to introduce continuous variables $\delta_k \in [0, 1]$ corresponding to the intervals, $k \in [K]$. As for the binary variables u_k , the continuous ones δ_k are also set to one when x exceeds t_k , which is enforced by the inequalities

$$\delta_{k+1} \leq u_k, \quad \text{for } k \in [K-1]. \quad (1)$$

The continuous variables even allow to model the value of x explicitly as

$$x = t_0 + \sum_{k=1}^K \delta_k (t_k - t_{k-1}), \quad (2)$$

whereas for the interpolation value w of f , we get

$$w = f(t_0) + \sum_{k=1}^K \delta_k (f(t_k) - f(t_{k-1})). \quad (3)$$

In conclusion, the incremental method poses a model for PWL approximation of the form

$$\begin{aligned}
& (1), (2), (3), \\
& \delta_1 \leq 1, \\
& u_k \leq \delta_k, \quad k \in [K-1], \\
& \delta_K \geq 0, \\
& u_k \in \{0, 1\}, \quad k \in [K-1],
\end{aligned} \tag{4}$$

where the edge cases are respected as well. Note that the binary variables are necessary to fix the δ -variables to their respective bounds such that only the relevant one is potentially fractional.

Since this main ingredient of “filling” or “incrementation” is often modeled via variables named δ , the method is also known by this respective name.

Note that system (4) models a PWL *approximation* of f such that $|w - f| \leq \varepsilon$ on \mathcal{D} . Thus, a simple replacement of each f_j in (P) with a corresponding w_j and (4) does in general not pose a relaxation (P_{rel}), but an approximated problem. Consequently, if the approximated problem is solved, its solution is not guaranteed to be also a solution of (P_ε). However, to retrieve a relaxation, we can define $\varepsilon' := \varepsilon/2$, compute a PWL approximation with respect to ε' , and shift the result for $\varepsilon/2$. In particular, the PWL approximation then ensures that $|w - f(x)| \leq \varepsilon'$ for all $x \in \mathcal{D}$. This implies that $w - \varepsilon' \leq f(x)$ and thus $|(w - \varepsilon') - f(x)| \leq |w - f(x)| + \varepsilon' \leq 2\varepsilon' = \varepsilon$. In other terms, a shift of the function values $f(t_k)$ in (3) by ε' is a shift in w and results in an underestimation – thus relaxation like (P_{rel}) – satisfying a tolerance of ε . Such a procedure for obtaining a PWL relaxation is performed throughout the present article and we refer to this relaxation technique simply by PWL.

2.4. Global One-sided Parabolic Model. The recently introduced approach of global one-sided parabolic (PARA) approximations and relaxations [26] aims to circumvent the use of binary variables as in PWL. For a given constraint function f , it computes an approximation \check{f} as the point-wise maximum of paraboloids, i.e., separable univariate quadratic functions, that underestimate f on \mathcal{D} individually and satisfy the given approximation tolerance. As we consider one dimensional constraint functions f only, we refer to this type of approximates as parabolas. Formally, for a set of $K \in \mathbb{N}$ parabolas $\{p_k\}_{k \in [K]}$, the approximation is $\check{f}(x) = \max_{k \in [K]} p_k(x)$ such that

$$f - \varepsilon \leq \check{f} \leq f \quad \text{on } \mathcal{D}. \tag{5}$$

In other terms, \check{f} represents an epigraph approximation of f . Due to the global underestimation, we can simply replace each constraint in (P) by a corresponding parabolic approximation and end up with (P_{rel}). Taking the presentation as ‘ \leq ’-constraints and the pointwise maximum into account, it even simplifies to the set of constraints $p_k(x) \leq y$, $k \in [K]$. This makes the modeling of PARA relaxations straightforward and does not rely on the use of binary variables.

It remains to clarify the computation of p_k in [26]. For a constraint function f and its domain $\mathcal{D} = [\underline{x}, \bar{x}]$, the approach requires a global Lipschitz constant $L > 0$ of f . This can be considered a weaker assumption in comparison to continuous differentiability, since maximizing $|f'|$ on \mathcal{D} gives L . Based on the magnitude of L , the approach in [26] performs a binary search on the number of parabolas K . During one search iteration, K is fixed and a MIP problem is constructed in which the coefficients of the parabolas are considered as variables. The problem’s constraints ensure the ε -approximation property of a solution, whereas the objective controls the global underestimation, i.e., the first and second inequality in (5), respectively. If the MIP problem is solved in a given time limit with objective of zero, the corresponding

parabolas fulfill (5) and the current K is decreased. Otherwise, the number of parabolas K is increased.

The weak assumptions necessary for the approach represent a clear advantage, as it leaves it applicable for a really broad class of constraint functions. However, relying on the solution of several MIP problems can be computationally challenging and results in function-domain- ε combinations that are not computable, see the comparison below in Section 3.2 for more details.

In fact, the article [26] introduces a theoretically valid as well as a more practical option of this approach. The latter circumvents some of the challenges by relaxing particular constraints of the MIP and by incorporating manual checks. Those changes turn it into a computationally more efficient version. Hence, we conduct the later comparison in Section 3.2 with respect to this version and refer to it as `practical-MIP`, following the original source.

3. COMPUTING PARABOLAS FAST

Inspired by the computation of PWL approximations, we introduce a novel method to compute PARA approximations for general nonlinear functions f in an iterative manner. We recall that f is assumed to be sufficiently continuous differentiable and defined on a domain $\mathcal{D} = [\underline{x}, \bar{x}]$. An explanation of the method and respective proofs of correctness are provided in Section 3.1. We refer this procedure as the PARA approximation method or shortly PARA. It is indeed able to compute parabolas for cases where the original method from [26] has failed, see Section 3.2. The computational performance even allows to conclude the present section with a comparison of number of approximates, i.e., parabolas and linear pieces, on general nonlinear functions that occur frequently in the MINLPLib [13].

3.1. Method. In contrast to the method in [26], we associate one parabola p_k , $k \in [K]$, with a certain domain $\mathcal{D}_k := [t_{k-1}, t_k]$, on which it fulfills the ε -approximation, i.e.,

$$f(x) - \varepsilon \leq p_k(x), \quad \text{for all } x \in \mathcal{D}_k. \quad (6)$$

To construct a global ε -approximation with all parabolas, they must satisfy the first inequality in (5) and we thus require

$$\bigcup_{k \in [K]} \mathcal{D}_k = \mathcal{D}. \quad (7)$$

Simultaneously, as described above, each p_k is supposed to serve as a global under-estimator of f , i.e.,

$$p_k(x) \leq f(x), \quad \text{for all } x \in \mathcal{D}. \quad (8)$$

This settles the description of the requirements.

Our new approach returns the parabolas “from left to right”, i.e., it computes a parabola which satisfies property (6) on $[\underline{x}, t_1] = [t_0, t_1]$, and then proceeds to $[t_1, t_2]$ until it reaches the upper bound \bar{x} with the final interval $[t_{K-1}, t_K] = [t_{K-1}, \bar{x}]$. Here, $K \geq 0$ indicates the necessary number of parabolas, which is determined a-posteriori. Such a procedure can be leveraged for computing PWL approximations as well, see Section 2.3.

Let’s turn to a particular iteration k and investigate the challenge at hand. The current lower bound is fixed at $t_{k-1} < \bar{x}$. To cover a large interval, on which p_k is a valid ε -approximation, we aim to maximize the next upper bound $t_k \leq \bar{x}$. Enforcing (6) and (8), we can formulate this as the semi-infinite optimization

problem

$$\begin{aligned} & \max_{t_k, \tilde{a}, \tilde{b}, \tilde{c}} t_k \\ \text{s.t. } & \tilde{a}x^2 + \tilde{b}x + \tilde{c} \geq f(x) - \varepsilon, & \text{for all } x \in [t_{k-1}, t_k] = \mathcal{D}_k, & (9a) \end{aligned}$$

$$\tilde{a}x^2 + \tilde{b}x + \tilde{c} \leq f(x), \quad \text{for all } x \in \mathcal{D}, \quad (9b)$$

where we define $t_0 = \underline{x}$ for \mathcal{D}_1 and $(\tilde{a}, \tilde{b}, \tilde{c})$ denote variables for the coefficients of p_k . A solution (a_k, b_k, c_k) to this problem then gives $p_k(x) := a_k x^2 + b_k x + c_k$, satisfying (6) and (8) by (9a) and (9b), respectively. However, the constraints (9) are infinitely many and thus require further treatment.

In a first attempt let us assume to have a fixed parabola p_k and a fixed upper bound t_k . Then, computing

$$\max_{x \in \mathcal{D}} p_k(x) - f(x) = \max_{x \in \mathcal{D}} a_k x^2 + b_k x + c_k - f(x), \quad (10)$$

and

$$\max_{x \in \mathcal{D}_k} f(x) - p_k(x) = \max_{x \in \mathcal{D}_k} f(x) - (a_k x^2 + b_k x + c_k), \quad (11)$$

can be considered computational tractable, since both problems require to maximize differences of continuously differentiable functions on a closed interval. This can be conducted by means of Newton-type methods, for instance.

Let z_k and z_k^ε denote the solutions for (10) and (11), respectively. Then, (9a) is fulfilled if and only if $f(z_k^\varepsilon) - p_k(z_k^\varepsilon) \leq \varepsilon$, and, analogously, (9b) is fulfilled if and only if $p_k(z_k) - f(z_k) \leq 0$. In the case that at least one of these inequalities does not hold, a decrease of the interval length $|\mathcal{D}_k|$, thus a shift of t_k towards t_{k-1} , and a new computation of p_k may resolve the issue.

Based on this observation, we propose a two-step or *inner-outer* approach. Let k be the current iteration index, then

- an outer loop tries to compute a maximal upper bound t_k for the current interval $[t_{k-1}, t_k]$, but iteratively reduces the value of t_k if the inner loop fails, shifting t_k in the direction of t_{k-1} , and
- an inner loop aims to find a feasible set of coefficients (a_k, b_k, c_k) , defining the current parabola p_k such that (9) hold true.

3.1.1. Inner Loop. We start our explanation with the inner loop. For ease of notation, we drop the iteration index k and thus write the current (local) domain $\mathcal{D}_k = \mathcal{D}_{\text{loc}} = [\underline{t}, \bar{t}]$ as well as $p_k(x) = p(x) = ax^2 + bx + c$.

Throughout the inner loop, we force p to cross $f - \varepsilon$ at the bounds of \mathcal{D}_{loc} . In particular, this can be expressed as

$$p(\underline{t}) = f(\underline{t}) - \varepsilon,$$

$$p(\bar{t}) = f(\bar{t}) - \varepsilon,$$

which reads in explicit form as

$$a\underline{t}^2 + b\underline{t} + c = f(\underline{t}) - \varepsilon, \quad (12a)$$

$$a\bar{t}^2 + b\bar{t} + c = f(\bar{t}) - \varepsilon. \quad (12b)$$

Neglecting (9b) for the moment, the intuition behind this measure is as follows: If the parabola p fulfills (9a) and simultaneously $p(\underline{t}) > f(\underline{t}) - \varepsilon$ or $p(\bar{t}) > f(\bar{t}) - \varepsilon$, the domain \mathcal{D}_{loc} could have been chosen larger.

Fixing p at the bounds of \mathcal{D}_{loc} reduces to original degrees of freedom when determining the three coefficients of p by two. In other words, given one of the

coefficients a , b , or c , this system uniquely determines the remaining two. To see this, assume coefficient a as fixed and rewrite the system (12) to $A\mathbf{v} = \mathbf{d}$, where

$$A = \begin{pmatrix} \underline{t} & 1 \\ \bar{t} & 1 \end{pmatrix}, \quad \mathbf{d} = \begin{pmatrix} f(\underline{t}) - \varepsilon - a\underline{t}^2 \\ f(\bar{t}) - \varepsilon - a\bar{t}^2 \end{pmatrix},$$

and $\mathbf{v} = (b \ c)^\top$. When $\mathcal{D}_{\text{loc}} \neq \emptyset$, so $\underline{t} < \bar{t}$, it holds $\det(A) = \underline{t} - \bar{t} < 0$ and the system always attains a unique solution.

Instead of fixing coefficient a to determine (b, c) , we combine (12) with (9) and can derive bounds to the quadratic coefficient a . This will allow to determine the existence of a feasible set of coefficients (a, b, c) and constitute the main ingredient of the inner loop. In the following, the derivation of bounds is formalized.

Lemma 1 (Bounds on a). *Let $f : \mathcal{D} \rightarrow \mathbb{R}$ be as above and $\text{int}(\mathcal{D}) \neq \emptyset$. Further, let $\varepsilon > 0$ and $\mathcal{D}_{\text{loc}} := [\underline{t}, \bar{t}] \subset \mathcal{D}$ such that $\underline{x} < \underline{t} < \bar{t} < \bar{x}$, implying $\text{int}(\mathcal{D}_{\text{loc}}) \neq \emptyset$. For a parabola $p(x) = ax^2 + bx + c$, assume (12). Then the following implications hold true.*

(a) Consider $\hat{x} \in \mathcal{D} \setminus \mathcal{D}_{\text{loc}}$. Then $p(\hat{x}) \leq f(\hat{x})$ if and only if

$$a \leq \frac{f(\hat{x}) - f(\underline{t}) + \varepsilon}{(\hat{x} - \underline{t})(\hat{x} - \bar{t})} - \frac{f(\bar{t}) - f(\underline{t})}{(\bar{t} - \underline{t})(\hat{x} - \bar{t})} =: A(\hat{x}).$$

(b) Consider $\hat{x} \in \text{int}(\mathcal{D}_{\text{loc}})$. Then $p(\hat{x}) \leq f(\hat{x})$ if and only if

$$a \geq \frac{f(\hat{x}) - f(\underline{t}) + \varepsilon}{(\hat{x} - \underline{t})(\hat{x} - \bar{t})} - \frac{f(\bar{t}) - f(\underline{t})}{(\bar{t} - \underline{t})(\hat{x} - \bar{t})} =: A(\hat{x}).$$

(c) Consider $\hat{x} \in \text{int}(\mathcal{D}_{\text{loc}})$. Then $p(\hat{x}) \geq f(\hat{x}) - \varepsilon$ if and only if

$$a \leq \frac{f(\hat{x}) - f(\underline{t})}{(\hat{x} - \underline{t})(\hat{x} - \bar{t})} - \frac{f(\bar{t}) - f(\underline{t})}{(\bar{t} - \underline{t})(\hat{x} - \bar{t})} =: B(\hat{x}).$$

Proof. As a preparatory step, we subtract (12a) from (12b) and get

$$a(\bar{t}^2 - \underline{t}^2) + b(\bar{t} - \underline{t}) = f(\bar{t}) - f(\underline{t}),$$

which is equivalent to

$$a(\bar{t} + \underline{t}) + b = \frac{f(\bar{t}) - f(\underline{t})}{\bar{t} - \underline{t}} \quad (13)$$

by division with $(\bar{t} - \underline{t})$. This preliminary work will support the proof for every of the three cases.

Case (a). Starting off, we write the condition from (a) explicitly, i.e.,

$$a\hat{x}^2 + b\hat{x} + c \leq f(\hat{x}).$$

By subtracting (12a), this is equivalent to

$$a(\hat{x}^2 - \underline{t}^2) + b(\hat{x} - \underline{t}) \leq f(\hat{x}) - f(\underline{t}) + \varepsilon.$$

Now, rearranging (13) for b and plugging the result into the former gives

$$\begin{aligned} & a(\hat{x}^2 - \underline{t}^2) + \left(\frac{f(\bar{t}) - f(\underline{t})}{\bar{t} - \underline{t}} - a(\bar{t} + \underline{t}) \right) (\hat{x} - \underline{t}) \leq f(\hat{x}) - f(\underline{t}) + \varepsilon \\ \iff & a(\hat{x}^2 - \underline{t}^2 - \bar{t}\hat{x} - \underline{t}\hat{x} + \bar{t}\underline{t} + \underline{t}^2) \leq f(\hat{x}) - f(\underline{t}) + \varepsilon - \frac{f(\bar{t}) - f(\underline{t})}{\bar{t} - \underline{t}} (\hat{x} - \underline{t}) \\ \iff & a(\hat{x} - \bar{t})(\hat{x} - \underline{t}) \leq f(\hat{x}) - f(\underline{t}) + \varepsilon - \frac{f(\bar{t}) - f(\underline{t})}{\bar{t} - \underline{t}} (\hat{x} - \underline{t}). \end{aligned}$$

As $\hat{x} \in \mathcal{D} \setminus \mathcal{D}_{\text{loc}}$, either $\hat{x} < \underline{t} < \bar{t}$ or $\underline{t} < \bar{t} < \hat{x}$. That is, $(\hat{x} - \bar{t})(\hat{x} - \underline{t}) > 0$ and thus division by this term does not change the direction of the inequality but leads to (a).

Case (b). This is analogous to case (a), however, the last division changes the sign of the inequality, as $\hat{x} \in \text{int}(\mathcal{D}_{\text{loc}})$ and thus $(\hat{x} - \bar{t})(\hat{x} - \underline{t}) < 0$.

Case (c). Again, we write the condition from (c) explicitly and get

$$a\hat{x}^2 + b\hat{x} + c \geq f(\hat{x}) - \varepsilon.$$

Subtraction of (12a) gives

$$a(\hat{x}^2 - \underline{t}^2) + b(\hat{x} - \underline{t}) \geq f(\hat{x}) - f(\underline{t}).$$

Following the strategy from previous cases and respecting that $\hat{x} \in \text{int}(\mathcal{D}_{\text{loc}})$ gives the desired inequality. \square

Lemma 1 implies that every point in $\mathcal{D} \setminus \mathcal{D}_{\text{loc}}$ implicitly gives an upper bound to the quadratic coefficient a and every point inside \mathcal{D}_{loc} even implies lower and upper bounds to a . Setting $\underline{a} \leftarrow \sup_{x \in \text{int}(\mathcal{D}_{\text{loc}})} A(x)$ and $\bar{a} \leftarrow \min(\inf_{x \in \mathcal{D} \setminus \mathcal{D}_{\text{loc}}} A(x), \inf_{x \in \mathcal{D}_{\text{loc}}} B(x))$, we ensure the existence of a feasible coefficient a (thus parabola) if and only if $\underline{a} \leq \bar{a}$. A feasible a can then be completed computing (b, c) by solving the linear system (12). In turn, if we know that $\underline{a} > \bar{a}$, there exists no feasible a and we need to shrink \mathcal{D}_{loc} in the outer loop.

The computation of the minima and maxima above to determine \underline{a} and \bar{a} is non-trivial, since the variable x appears in the denominator of a fraction, especially in a term that converges to infinity. Hence, we compute these bounds iteratively, starting with some initial values \underline{a}_0 and \bar{a}_0 . In fact, as any $a \in [\underline{a}, \bar{a}]$ is valid, we initialize \underline{a}_0 with negative infinity and always set a to be the current upper bound. This will facilitate the presentation of the method and showing its correctness. However, it remains to find a value for \bar{a}_0 , which can also be derived by the results of Lemma 1 as mentioned below.

Remark 2. Consider a point $x \in \text{int}(\mathcal{D}_{\text{loc}})$ and Lemma 1(c). If $x \rightarrow \underline{t}$, the inequality bounding coefficient a turns into

$$a \leq \frac{f'(\underline{t})}{\underline{t} - \bar{t}} + \frac{f(\bar{t}) - f(\underline{t})}{(\bar{t} - \underline{t})^2} = (f(\bar{t}) - f(\underline{t}) + (\underline{t} - \bar{t})f'(\underline{t})) / (\bar{t} - \underline{t})^2.$$

This directly gives an upper bound to a , which can be used for \bar{a}_0 .

For the case $x \rightarrow \bar{t}$, we first need to rewrite $B(x)$. By respecting that

$$D := \frac{1}{(x - \underline{t})(x - \bar{t})} - \frac{1}{(\bar{t} - \underline{t})(x - \bar{t})} = -\frac{1}{(\bar{t} - \underline{t})(x - \underline{t})},$$

we can derive that

$$\begin{aligned} B(x) &= \frac{f(x) - f(\underline{t}) - f(\bar{t}) + f(\bar{t})}{(x - \underline{t})(x - \bar{t})} - \frac{f(\bar{t}) - f(\underline{t})}{(\bar{t} - \underline{t})(x - \bar{t})} \\ &= \frac{f(x) - f(\bar{t})}{(x - \underline{t})(x - \bar{t})} + (f(\bar{t}) - f(\underline{t}))D \\ &= \frac{f(x) - f(\bar{t})}{(x - \underline{t})(x - \bar{t})} - \frac{f(\bar{t}) - f(\underline{t})}{(\bar{t} - \underline{t})(x - \underline{t})}. \end{aligned}$$

Then, considering $x \rightarrow \bar{t}$ for $x \in \text{int}(\mathcal{D}_{\text{loc}})$, Lemma 1(c) provides that

$$a \leq (f(\underline{t}) - f(\bar{t}) + (\bar{t} - \underline{t})f'(\bar{t})) / (\bar{t} - \underline{t})^2.$$

Taking the minimum of both those upper bounds, leads to \bar{a}_0 for our inner loop.

After initializing the quadratic coefficient a , the remaining coefficients (b, c) can be computed by solving (12). Then, the inner loop tests for (6) and (8) by

computing (10) on $\mathcal{D} \setminus \mathcal{D}_{\text{loc}}$ and \mathcal{D}_{loc} separately, as well as (11) on \mathcal{D}_{loc} . Explicitly, for a fixed parabola p , this is

$$\max_{x \in \mathcal{D} \setminus \mathcal{D}_{\text{loc}}} p(x) - f(x), \quad (14a)$$

$$\max_{x \in \text{int}(\mathcal{D}_{\text{loc}})} p(x) - f(x), \quad (14b)$$

$$\max_{x \in \text{int}(\mathcal{D}_{\text{loc}})} f(x) - p(x) - \varepsilon. \quad (14c)$$

We denote the solutions by x^1, x^2, x^3 and their values by v_1, v_2, v_3 , respectively. If $v_{\max} := \max\{v_1, v_2, v_3\}$ exceeds the threshold of zero, the current choice of coefficient a is infeasible and x^1, x^2, x^3 are considered as candidates for “ \hat{x} ” in Lemma 1, implying an update of the current bounds \underline{a}_l and \bar{a}_l on a .

The process is iterated until the bounds are contradictory, signaling the absence of a feasible triple (a, b, c) , or until the constraints (9) are satisfied. This process is summarized in Method 1. Arrows are always pointing towards the object that is returned by this step.

Method 1 Inner loop – Computing (a, b, c) .

Input: (Local) Interval bounds \underline{t} and \bar{t} such that $\underline{t} < \bar{t}$.

Output: Coefficients (a, b, c) defining p satisfying (9) or “Infeasible”.

- 1: Initialize \bar{a}_0 according to Remark 2, $\underline{a}_0 \leftarrow -\infty$, and $l \leftarrow 0$.
 - 2: Set $a_0 \leftarrow \bar{a}_l$ and compute (b_l, c_l) according to (12).
 - 3: **while** $\underline{a}_l \leq \bar{a}_l$ **do**
 - 4: Compute (14) $\rightarrow x^1, x^2, x^3, v_{\max}$.
 - 5: **if** $v_{\max} \leq 0$ **then**
 - 6: **return** (a_l, b_l, c_l) .
 - 7: **end if**
 - 8: Update \underline{a}_{l+1} and \bar{a}_{l+1} with x^1, x^2, x^3 according to Lemma 1.
 - 9: Increment $l \leftarrow l + 1$.
 - 10: Set $a_l \leftarrow \bar{a}_l$ and compute (b_l, c_l) according to (12).
 - 11: **end while**
 - 12: **return** “Infeasible”.
-

After its presentation, we continue by formally showing the correct mode of operation of the inner loop.

Theorem 3 (Correctness of Method 1). *If there exists a solution (a, b, c) fulfilling (9) and (12), Method 1 returns one or converges to it. Otherwise, it returns that there is no such solution.*

The following provides a proof sketch, for which the details can be found in Appendix A.1.

Proof. By leveraging Lemma 1 the existence of finite bounds $\underline{a} \leq \bar{a}$ is equivalent to the existence of a solution (a, b, c) . This represents the main ingredient.

If there exists a solution, the condition of the while-loop is always met. Since a_l in iteration l is chosen to be the current \bar{a}_l , also $a_l \geq \underline{a}$ for all l . By Lemma 1, it thus always holds that $p \leq f$ on $\text{int}(\mathcal{D}_{\text{loc}})$. The remaining cases, $p \leq f$ on $\mathcal{D} \setminus \mathcal{D}_{\text{loc}}$ and $p \geq f - \varepsilon$ on $\text{int}(\mathcal{D}_{\text{loc}})$, are proven following the same strategy: We use (12) to write down a parameterized version of parabola p in the quadratic coefficient a . This allows us to show convergence by contradiction. \square

3.1.2. *Outer Loop.* While the inner loop computes an approximating parabola for a given interval or asserts with its impossibility, it remains to consider the interval bounds. We propose to start with the global interval $[t_0, t_1] := [\underline{x}, \bar{x}]$ and consecutively shift t_1 toward t_0 , until a suitable parabola can be computed by the inner loop. After storing the parabola and the associated domain $[t_0, t_1]$, the remaining interval $[t_1, \bar{x}]$ is considered next. This is iterated until K parabolas p_k with their associated domains \mathcal{D}_k are computed, covering the entire global domain \mathcal{D} , i.e., fulfilling (7). This procedure is presented in pseudocode in Method 2.

Method 2 Outer loop – Computing \mathcal{D}_k

Input: (Global) Domain $\mathcal{D} = [\underline{x}, \bar{x}] \neq \emptyset$, approximation tolerance $\varepsilon > 0$.

Output: A set of coefficients (a_k, b_k, c_k) defining p_k , $k \in [K]$, $K \in \mathbb{N}$, such that (5).

```

1: Initialize  $k \leftarrow 1$ ,  $t_0 \leftarrow \underline{x}$ ,  $t_1 \leftarrow \bar{x}$ .
2: while  $t_{k-1} < \bar{x}$  do
3:   Call Method 1 on  $[t_{k-1}, t_k] \rightarrow (a, b, c)$  or “Infeasible”.
4:   if “Infeasible” then
5:     Shift  $t_k$  towards  $t_{k-1}$ .
6:   else
7:     Store  $(a_k, b_k, c_k)$ .
8:     Set  $t_{k+1} \leftarrow \bar{x}$  and increment  $k \leftarrow k + 1$ .
9:   end if
10: end while
11: return Parameters  $(a_k, b_k, c_k)$  for  $k \in [k]$ .

```

Depending on the type of shift applied in Step 5, the number of parabolas and thus iterations varies. We want to briefly discuss this effect by supposing a shift in form of a convex combination, i.e., $t_k \leftarrow \lambda t_{k-1} + (1 - \lambda)t_k$ for $\lambda \in (0, 1)$. If λ is near 1, the shift is strong towards t_{k-1} and the length of the current interval \mathcal{D}_k is decreased rapidly. In consequence, it is likely to find a suitable parabola with (6) and (8) after only a couple of “Infeasible”-iterations of the inner loop. However, it takes a considerable number K of intervals – thus parabolas – to cover the entire domain, i.e., to reach (7). In turn, a value of λ close to 0 results in the opposite effect, potentially computing a small number of parabolas – thus few quadratic constraints for the PARA relaxation – but for a certain computational cost.

The specific number of calls of the inner loop depends on the function f and its domain \mathcal{D} to be considered, as well as on the value of λ . From the theoretical side, however, it remains to show that Method 2 converges *at all*. In the following, we will demonstrate it, supposing the shift in Step 5 to be a true decrease of the interval length of \mathcal{D}_k that still ensures $|\mathcal{D}_k| > 0$. In particular, we show that for small enough domains \mathcal{D}_k , there exists a respective solution p_k . This allows to derive by Theorem 3 that the inner loop at least converges to such a solution. Considering numerical precision and thus finiteness of the inner loop, we can conclude that Method 2 terminates.

Note that we will only leverage Lipschitz continuity of our function f for this proof. As noted in Section 2.4, a global Lipschitz constant L can be computed as (an upper bound to) $\max\{|f'(x)| \mid x \in \mathcal{D}\}$, i.e., the assumptions of the theorem apply to the given setup. Keeping the assumptions on f low, however, allows for wider application and a comparison of the proof techniques to the ones in [26].

Theorem 4 (Correctness of Method 2). *Let $\mathcal{D} \neq \emptyset$, $f : \mathcal{D} \rightarrow \mathbb{R}$ be globally Lipschitz continuous with $L > 0$ and $\varepsilon > 0$. Then, for any interval length $\Delta > 0$ with $\Delta \leq \varepsilon/(3L)$ and $|\mathcal{D}|/\Delta \in \mathbb{N}$, one can choose \mathcal{D}_k as a partition of \mathcal{D} with $|\mathcal{D}_k| = \Delta$*

	domain \mathcal{D}					
exp	$[-5, -2]$	$[-2, 2]$	$[-5, 2]$	$[2, 5]$	$[-2, 5]$	$[-5, 5]$
sin	$[-\frac{\pi}{2}, \frac{\pi}{2}]$	$[\frac{\pi}{2}, \frac{3\pi}{2}]$	$[-\frac{\pi}{2}, \frac{3\pi}{2}]$	$[0, \pi]$	$[\pi, 2\pi]$	$[0, 2\pi]$

TABLE 1. Function-domain combinations to approximate with Method 2 for comparison with [26].

and by setting $a_k = -4L/\Delta$ there exist parabolas $p_k(x) = a_k x^2 + b_k + c_k$, $k \in [|\mathcal{D}|/\Delta]$, fulfilling the properties (6) and (8).

The following provides a proof sketch, since the full proof is of technical nature. Details can be found in Appendix A.2.

Proof. For a given local interval \mathcal{D}_{loc} with length Δ , we show the existence of a parabola p such that

- a) $p(x) \geq f(x) - \varepsilon$ on \mathcal{D}_{loc} ,
- b) $p(x) \leq f(x)$ on \mathcal{D}_{loc} , and
- c) $p(x) \leq f(x)$ on $\mathcal{D} \setminus \mathcal{D}_{\text{loc}}$.

For case a), we make use of Lemma 1 and show that $\tilde{a} \leq B(x)$ for all $x \in \text{int}(\mathcal{D}_{\text{loc}})$. Cases b) and c) are straightforward, using the Lipschitz continuity and the assumptions to Δ . Denoting the mid point of \mathcal{D}_{loc} as \tilde{t} , all three cases distinguish $x \leq \tilde{t}$ and $x \geq \tilde{t}$.

□

3.2. Computational Results. We aim to complement the explanation of PARA in the previous section with a performance evaluation compared to the existing method and a quantitative comparison to PWL. Our implementation is conducted in Python 3.11.8 and can be found here: <https://github.com/adriangoess/pwl-vs-para>. For the shift in Method 2 Step 5, we use a convex combination $t_k \leftarrow (1 - \lambda)t_{k-1} + \lambda t_k$, where $\lambda = 0.9$.

3.2.1. Comparison to Existing Method. To the best of our knowledge, the only method achieving the same type of PARA approximation is presented in [26] and has been described in Section 2.4. Following the original source, we refer to the method as `practical-MIP`. The method is leveraged to compute PARA approximations on different domains and varying tolerance for different types of functions, including the sine and the exponential function. For a successful run, the resulting number of parabolas is reported. However, there also exist cases for which the `practical-MIP` approach was not able to generate a result.

We compare the number of (un)successful runs and the number of resulting parabolas. For sin and exp, we consider the same intervals and tolerances as in [26], which are summarized in Table 1.

For the comparison, we leverage a similar type of table as used in [26]. The results regarding the sine function are then summarized in Table 2. We denote the number of parabolas computed by `practical-MIP` – if any – in brackets and highlight the smaller such number in bold.

First of all, for the cases where either method is successful, we observe mixed results. There is no consistently superior method in terms of less parabolas, but in some cases Method 2 finds a significantly lower number. For a potential explanation of such a phenomenon, we have to take into account that `practical-MIP` relies on a binary search in this quantity. That is, after every run that reports the **MIP!** (**MIP!**) problem to be infeasible or hits the time limit, the search procedure doubles the number of parabolas and restarts. Hence, it may return high intermediate numbers as they are the best known when terminating after a fixed number of tries.

\mathcal{D}	ε							
	10^0	10^{-1}	10^{-2}	10^{-3}	10^0	10^{-1}	10^{-2}	10^{-3}
$[-\pi/2, \pi/2]$	1 (1)	3 (3)	7 (9)	22	1 (1)	3 (3)	7 (8)	22
$[\pi/2, 3\pi/2]$	1 (1)	3 (3)	7 (8)	22	1 (1)	3 (3)	7 (8)	22
$[-\pi/2, 3\pi/2]$	2 (1)	5 (5)	14 (47)	44	1 (1)	5 (3)	17 (13)	51
$[0, \pi]$	1 (1)	2 (1)	5 (5)	16 (40)	1 (1)	1 (1)	5 (3)	16 (16)
$[\pi, 2\pi]$	1 (1)	1 (1)	5 (3)	16 (32)	1 (1)	2 (1)	5 (5)	16
$[0, 2\pi]$	2 (2)	4 (5)	14 (24)	44	2 (2)	4 (5)	14 (44)	44
	above				below			

TABLE 2. Number of parabolas to approximate sin with Method 2 (practical-MIP).

\mathcal{D}	ε							
	10^0	10^{-1}	10^{-2}	10^{-3}	10^0	10^{-1}	10^{-2}	10^{-3}
$[-5, -2]$	1 (1)	1 (1)	2 (2)	5 (5)	1 (1)	1 (1)	2 (2)	5 (8)
$[-2, 2]$	2 (2)	5 (5)	15 (32)	47	2 (2)	4 (4)	13 (20)	39
$[-5, 2]$	3 (3)	7 (8)	23 (81)	70	2 (2)	6 (6)	16 (56)	51
$[2, 5]$	6	16	50	158	5 (5)	14 (20)	44	137
$[-2, 5]$	10	31	99	313	8	23	72	225
$[-5, 5]$	13	39	122	382	9	26	79	251
	above				below			

TABLE 3. Number of parabolas to approximate exp with Method 2 (practical-MIP).

For the other cases, we see that Method 2 is able to return an approximating set of parabolas in all cases, for which practical-MIP has failed, especially refer to the columns with a tolerance of 10^{-3} . The generality of the setup in practical-MIP allows for wide application, but the underlying MIP problem requires a number of (binary) variables growing linearly in the tolerance and the global Lipschitz constant. The resulting MIP problems may not be solved in a considerable time limit, as specified in [26]. Method 2, in contrast, can make use of more restrictive properties like continuous differentiability (when computing the maxima in (14)) to return approximations on larger domains. Surely, a tighter tolerance requires more parabolas and thus more computations. However, the respective effort seems to be manageable.

For the exponential function, both effects are observed in even greater extent, compare Table 3. For cases, where both methods are successful, Method 2 returns at most as much approximating parabolas as practical-MIP. That is, it outperforms practical-MIP on every domain-tolerance combination. In the other cases, practical-MIP struggles on domains with a large upper bound, since this implies a large global Lipschitz constant as explained in [26]. The obstacle seems to be circumvented with Method 2. Again, this results from avoiding to solve several (large) MIP problems, but instead only computing maxima on simple intervals.

3.2.2. *Number of Parabolas and Linear Pieces.* Besides a computational comparison of the PARA and the PWL relaxation technique on MINLP problems in terms of run time, one might also wonder about the number of approximates – parabolas or linear pieces. In a relaxation each such requires an additional constraint and, in

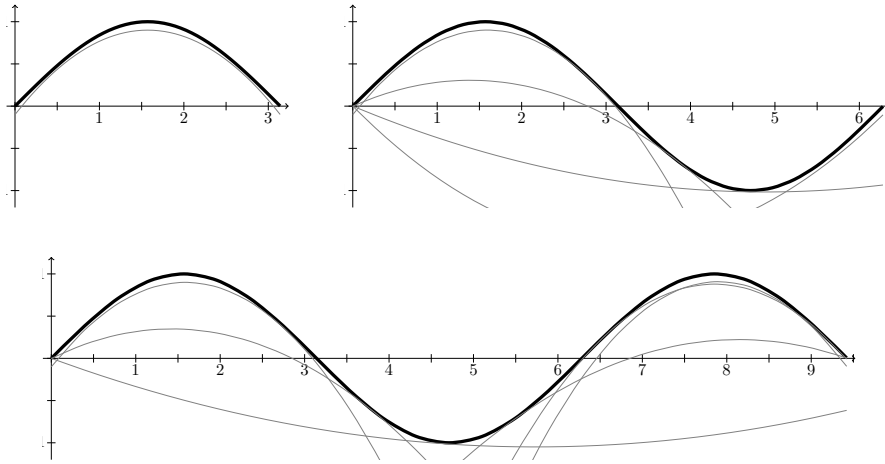


FIGURE 1. PARA approximations of \sin with $\varepsilon = 0.1$ on $[0, \ell\pi]$ for $\ell \in \{1, 2, 3\}$ by 1, 4, 6 parabolas, respectively.

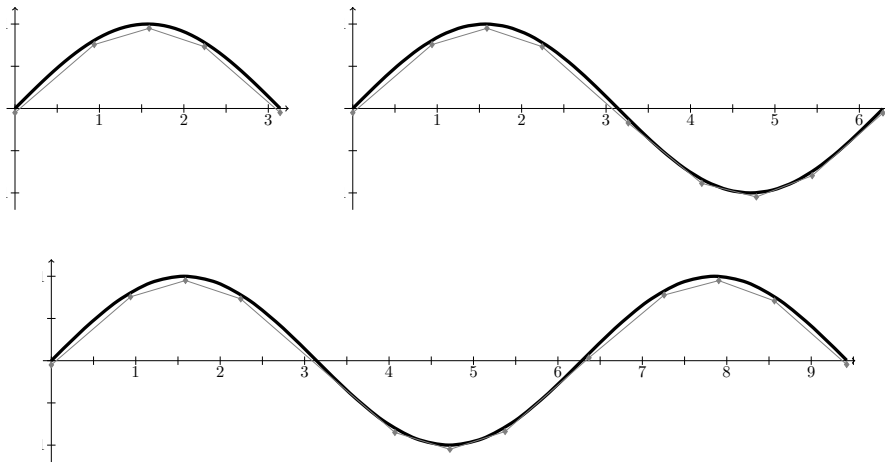


FIGURE 2. PWL approximations of \sin on with $\varepsilon = 0.1$ on $[0, \ell\pi]$ for $\ell \in \{1, 2, 3\}$ with 4, 8, 12 pieces, respectively.

case of PWL, additional variables. We aim to answer the question computationally, considering a fixed tolerance of $\varepsilon = 0.1$ and varying domains for fixed functions. The computation of the linear pieces follows the explanation in Section 2.3 and is performed by slightly modifying the code provided in [9]. As explained, it is run with a tolerance of $\varepsilon/2$ and the returned approximation is then shifted by $\varepsilon/2$ to receive a true relaxation. For computing the parabolas, we use Method 2.

At first, we take $f = \sin$ into account and investigate the number of approximates on $[0, \ell\pi]$ for $\ell \in \{1, 2, 3\}$. For PARA, we get 1, 6, 8, parabolas, respectively, which is visualized in Figure 1. For PWL, we end up with 4, 8, 12 linear pieces as shown in Figure 2. Such a linear growth of the number of pieces is to be expected when considering a periodic function like \sin .

Contemplating the approximations on $[0, \pi]$, the \sin function is reminiscent of a concave parabola and thus requires a lower number of such. However, for the convex

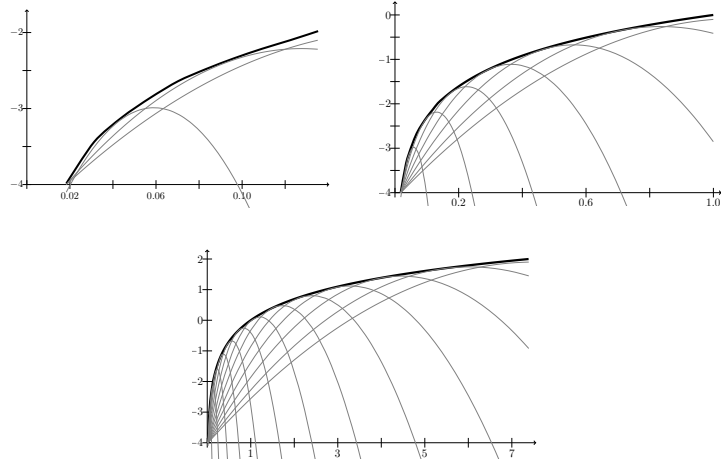


FIGURE 3. PARA approximations of \ln with $\varepsilon = 0.1$ on $[e^{-4}, e^{2\ell}]$ for $\ell \in \{-1, 0, 1\}$ with 3, 7, 13 parabolas, respectively.

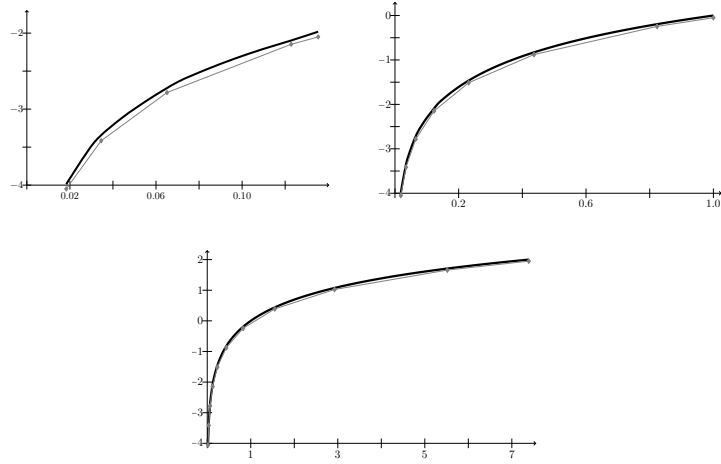


FIGURE 4. PWL approximations of \ln with $\varepsilon = 0.1$ on $[e^{-4}, e^{2\ell}]$ for $\ell \in \{-1, 0, 1\}$ with 4, 7, 10 pieces, respectively.

part, PARA needs to respect the global underestimation (8) and accordingly a larger domain. Hence, it has not been obvious to us that a lower number of parabolas is sufficient even when enlarging the respective domain. In conclusion, PARA seems to approximate the sine function with quite a few approximating parabolas, requiring even less approximates than PWL.

In the search for other examples, we deem a function that combines high slope and an asymptotically linear part as a challenge for PARA. Hence, we consider the natural logarithm \ln on a variety of domains, in particular $[e^{-4}, e^{2\ell}]$ for $\ell \in \{-1, 0, 1\}$. The corresponding illustrations for the PARA and PWL approximations can be found in Figure 3 and Figure 4, respectively.

As before, PARA requires less approximates for the smallest interval, i.e., 3 parabolas versus 4 linear pieces. However, when we enlarge the function domain, the number of parabolas (7 and 13) increasingly exceeds the number of linear pieces (7 and

10). Indeed, this results from the described form of \ln and the property of globally underestimating the function with every parabola on the entire domain.

In conclusion, those two examples showcase that there is no general statement about the necessary number of linear pieces with respect to the parabolas. Nonetheless, the investigation provides an intuition about it.

4. COMPARISON OF RELAXATION TECHNIQUES

Using the PARA method from the previous section, we are enabled to compute PARA relaxations for general nonlinear, one-dimensional constraint functions on relatively large domains and up to small approximation tolerances. It allows for a comparison with the PWL relaxation technique. In particular, we construct ε -relaxations in the form of (P_{rel}) for varying values of the approximation tolerance ε using either technique. If a solver can compute an optimal solution to such a relaxation, this solution is also optimal for the corresponding problem (P_ε) . Hence, we can simply compare the run times achieved with either relaxation, fixing a tolerance ε . The code can again be found in <https://github.com/adriangoess/pwl-vs-para>.

4.1. Test set. For a potential test set, we consider the MINLPLib [13] with 1595 MINLP instances. First of all, we aim to leverage the expression tree structure explained in Section 2.2 and thus restrict to the instances available in OSiL format [23], which are all but one. Second, we only consider instances that feature at least one exponential, natural logarithm, sine, or cosine function, since we focus on their relaxation. We remain with an intermediate subset of 235 instances.

Besides this formal filtering we need to respect the characteristics of the relaxation techniques. Particularly, either one requires finite bounds for the constraint function to relax and the size of the resulting relaxations, i.e., the number of linear pieces or parabolas, depends on the size of the finite domain. Typically, the function domains in such instances are sterile, meaning that a part of the domain is not even feasible, considering function properties or the relationships in the overall problem. That is, we can tighten the domains by applying a presolving step. For this, we make use of SCIP 10.0 [28]. It already incorporates the functionality of pure presolving which we apply with the settings `constraints/and/linearize=TRUE` and `presolving/gateextraction/maxrounds=0`. These ensure to avoid so-called “and”-constraints in the resulting problems, which is necessary to write them in respective format.

With respect to format, SCIP has a reader-functionality for OSiL, but no writer-functionality, so we write in GAMS format and re-convert to OSiL using GAMS 51.3.0 [15]. Hereby, we ruled out two instances containing the entropy function, since they could not be converted accordingly. In addition, we had to rule out five instances where this conversion step failed and we could not resolve its issue.

Despite the presolving step, however, there remain instances featuring general nonlinear constraint functions defined on infinite domains or domains that we consider numerically challenging. Specifically, the latter may either contain very large absolute values and/or force the corresponding function to be very close to zero or tremendously large. This can lead to numerical errors when constructing the relaxations or even solving such problems. Hence we restrict to instances that show the domain of an exponential function to be a subset of $[-5 \cdot 10^5, 10]$ and the domain of a natural logarithm to be a subset of $[10^{-7}, 10^7]$. We remain with a final test set of 174 instances.

4.2. Computational Setup. For all instances in our test set, we analyze the occurring general nonlinear, one-dimensional functions with their presolved domains.

For computing PWL approximations, we consider each function-domain combination and compute a respective relaxation as detailed in Section 2.3 using a slightly manipulated version of the code provided in [9]. The manipulation consists of relaxing only the general nonlinear functions and writing the respective problem in GAMS format.

For PARA, we stick to the paradigm introduced in [26], which advocates the use of PARA approximations in terms of a look-up table. That is, we cluster the bounds obtained in the presolved instances for the general nonlinear functions and compute the corresponding parabolas beforehand. In particular, for the exponential function, we round a lower bound down to the next multiplicative order of magnitude if its less than -1, else to the first digit. This ensures to cluster lower bounds with similar function value, i.e., small lower bounds, into the same subintervals, while respecting larger differences with increasing bound. To give an example, -132 is rounded to -200, whereas -0.456 to -0.5. For the upper bound, we proceed similarly for the same reason, but round it up and consider the first digit if it is less or equal 0, but the second digit if it is positive. For the natural logarithm, a reversed procedure is conducted: For a bound between $10^{\ell-1}$ and 10^ℓ , $\ell \in \mathbb{Z}$, it is rounded to the next multiplicative of $10^{\ell-1}$. This is capped for the lower bound with $\ell \leq 3$ and for the upper bound with $\ell \geq -1$, where the corresponding multiplicative of $\ell = 3$ and $\ell = -1$ is considered, respectively. For the sine and cosine function, the bounds are simply grouped in multiplicatives of 0.1 for domains with a length of less or equal 4π , otherwise we concatenate an approximation on an entire period by shifting.

We perform the upper procedure for both relaxation techniques for varying approximation tolerance $\varepsilon \in \{10^0, 10^{-1}, 10^{-2}, 10^{-3}, 10^{-4}\}$. Each problem is written in GAMS format and converted as explained above. The resulting problems are solved by leveraging SCIP 10.0 once again. All those solving processes are carried out on single nodes with Intel Xeon Gold 6326 “Ice Lake” multicore processors with 2.9GHz per core. The accessible RAM per node is set to 32GB, where SCIP is restricted to only use 30GB, avoiding issues with reading/modeling overhead. For every problem, we impose a time limit of 4h equaling 14400s.

Note that there occurred issues in conversion as well as memory issues and numerical troubles. If one or both resulting relaxations were affected by one such, we removed them from further consideration. This decreased the number of instances for the comparison to 150.

4.3. “Clash” of Relaxations. As laid out before, we can restrict our comparison to sole run time. For this, we start by comparing the number of faster runs per tolerance ε . Two runs on the same instance are considered equally fast, if the solution time varies by less than 5s. Figure 5 depicts the number of instances for which the respective relaxation approach could be solved in less time, for decreasing tolerance from left to right. The lines indicate trends.

We observe that the number of instances without a clear winner is comparably high, decreasing with lower approximation tolerance. On the one hand, this is an effect by hard instances on which both relaxations hit the time limit throughout all tolerances ε . On the other hand, small-sized instances require quite simple relaxations and are thus solved in a short amount of time for either relaxation. The latter effect is reduced with very small tolerance, since it requires a considerable number of parabolas or linear pieces, causing the solving time to deviate significantly.

For the comparison of PARA and PWL, we see a great favor towards the PWL approach for large tolerances. In those cases, PWL requires none to only a few additional binary variables along the linear constraints and thus seems to be more tractable than, potentially non-convex, quadratic constraints. For smaller tolerance, however, the advantage of not introducing additional binary variables seems to

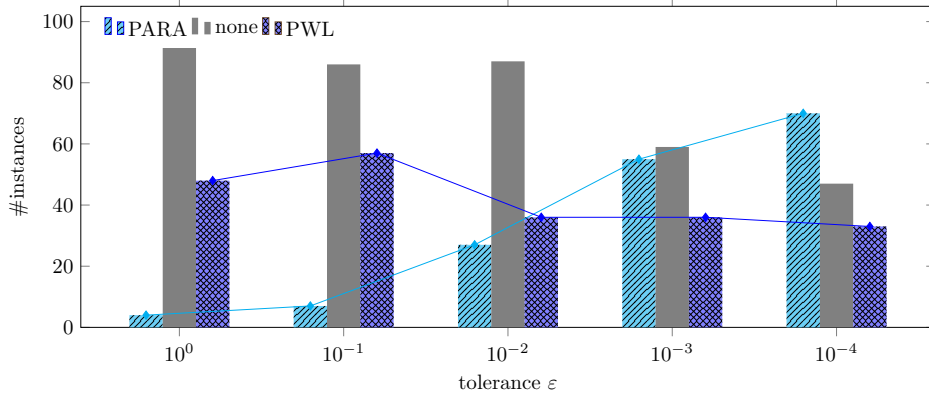


FIGURE 5. Number (#) of instances solved faster by PARA or PWL per tolerance ε .

outweigh the nonlinearity of the parabolic – thus quadratic – constraints. The internal expressions in SCIP seem to handle additional similar-shaped constraints quite well in comparison.

In order to investigate this phenomenon to greater extent, we also evaluate the results in form of performance profiles using the software of [39]. Such performance profiles compare the the run time of the solver on a specific relaxation to the fastest/shortest run time. In particular, they depict the fraction of problems solved within a factor (the performance ratio) of the fastest run available. For a fair comparison, we also include a base run, i.e., solving the presolved instances without reformulation or relaxation. The profiles are showcased for the extreme and intermediate cases $\varepsilon \in \{10^0, 10^{-2}, 10^{-4}\}$ in Figure 6, Figure 7, and Figure 8, respectively.

For the highest tolerance $\varepsilon = 10^0$ in Figure 6, we can see the aforementioned strength of PWL. Few binary variables and linear constraints are tractable in modern solvers. Interestingly, the introduction of PARA constraints is only a benefit up to a certain ratio and already falls behind later on. Such effects can be caused by approximating already convex constraints, e.g., an underestimation of the exponential function, by multiple quadratic constraints. Note that this was not ruled out a-priorily to allow the comparison against PWL.

For $\varepsilon = 10^{-2}$ and $\varepsilon = 10^{-4}$, we first observe that the base run is almost always the fastest approach, see Figure 7 and Figure 8, respectively. This may be a consequence by the lack of adaptivity for the presented techniques. In particular, a solver refines the underlying relaxation locally to avoid large overhead and thus adaptively incorporates additional relaxation constraints. This is the default for piecewise linear relaxations in modern solvers, yet there exists no implementation for the parabolic approach. Since the latter requires new theoretical foundations and implementations, we consider it as out of scope for the current paper and take up on it in Section 5.

Note that the base run is included to provide an insight about the original difficulty of the instances. However, the focus of this article truly lies in a comparison of the relaxation techniques in terms of computational efficacy.

Turning to this comparison of PARA and PWL in those cases, we can see that for $\varepsilon = 10^{-2}$, PARA already shows a better performance for ratios up to four, before PWL takes over. For $\varepsilon = 10^{-4}$ this is even increased up until around a ratio of 300, which is quite high. These observations reinforce the effect described above:

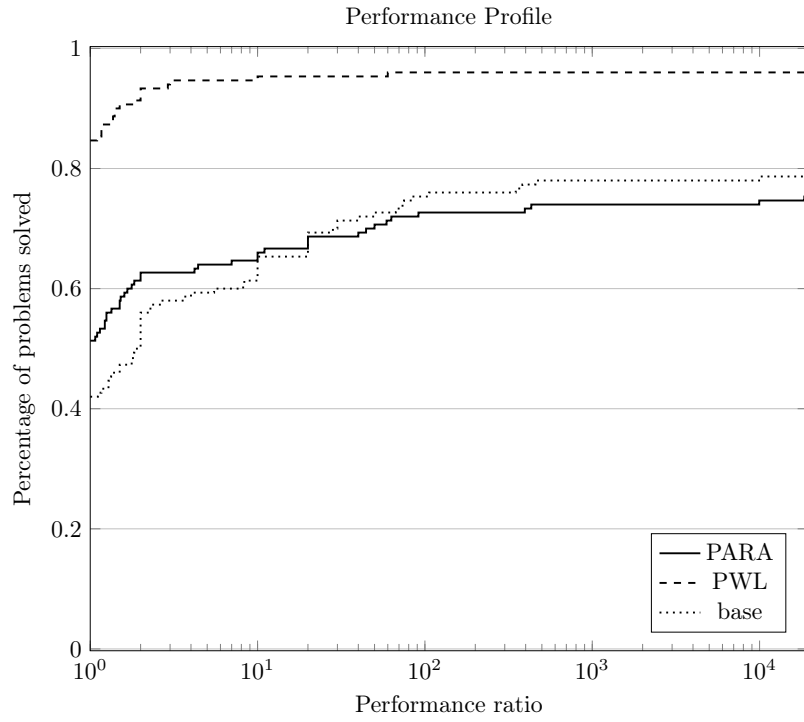


FIGURE 6. PARA and PWL for $\varepsilon = 10^0$ and base runs.

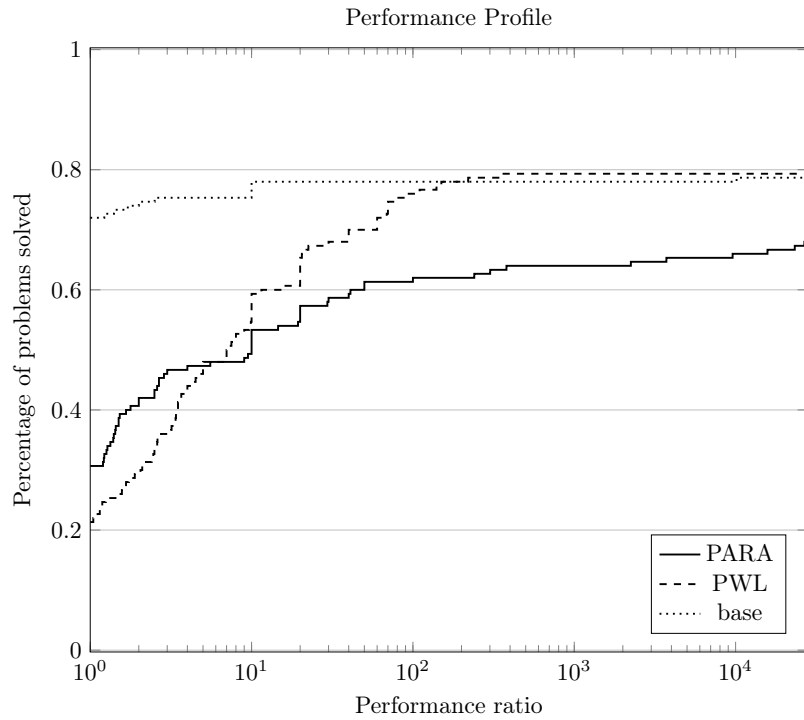


FIGURE 7. PARA and PWL for $\varepsilon = 10^{-2}$ and base runs.

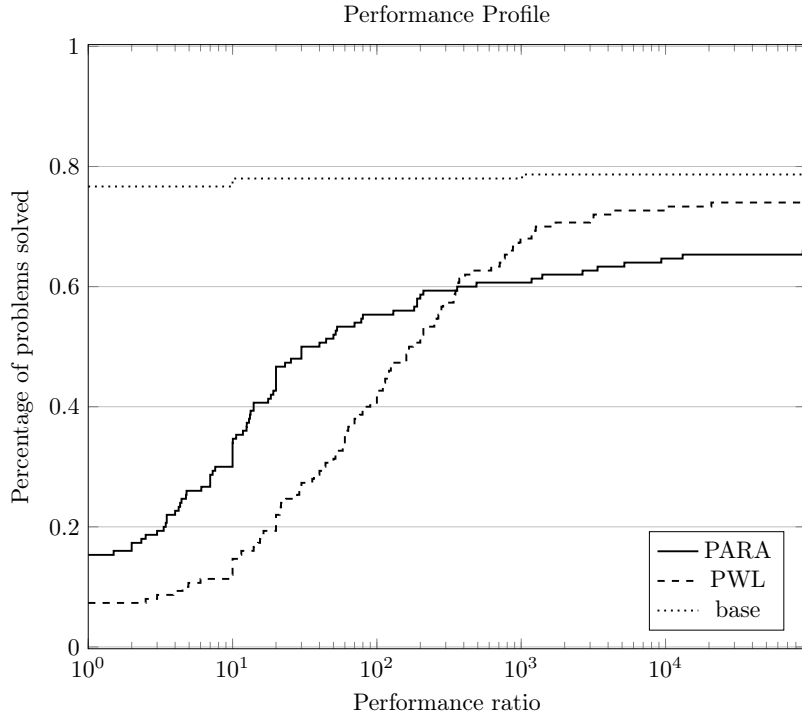


FIGURE 8. PARA and PWL for $\varepsilon = 10^{-4}$ and base runs.

For small tolerances, (non-convex) quadratic constraints can be leveraged more efficiently than additional binary variables and linear pieces, but only up to a certain point.

In the light of Section 3.2.2, instances that feature sine or cosine functions and not the natural logarithm, maybe be especially beneficial for the PARA approach. Such problems occur in the optimization of power networks, see [1, 7, 24], for instance. Hence, we consider a subset containing only instances with at least one sine or cosine function, which comprises exactly those instances without a natural logarithm nonlinearity (on our test set). This results in a subset of 33 instances.

We conduct the same comparison as before and display the number of instances with faster runs using the respective approach in Figure 9. As expected, the previously detected effects are enhanced. Relaxations by PARA are solved faster for all but one instances for tolerances $\varepsilon = 10^{-2}$ and below.

Turning to the performance profile for $\varepsilon = 10^0$ in Figure 10, we notice that both relaxations return instances being solved faster than the base ones. Though PWL relaxations still require less time than PARA, the effect is mitigated in comparison to the entire test set.

Now, for $\varepsilon = 10^{-2}$, PARA already consistently outperforms PWL and even is as least as fast as the base runs, not respecting any kind of adaptivity, see Figure 11. Whereas the exceed in performance between the relaxation techniques prevails for even smaller tolerance of $\varepsilon = 10^{-4}$ in Figure 12, we observe that up until a factor of 100, the base runs are faster. We dedicate this to the same effects mentioned above.

Suppose we try to solve instances that mainly feature (co)sine functions in their constraints and require medium to small tolerances. Then, the above results demonstrate that PARA relaxations can provide problem formulations that are being solved faster than tackling the original problem with a stand-alone solver.

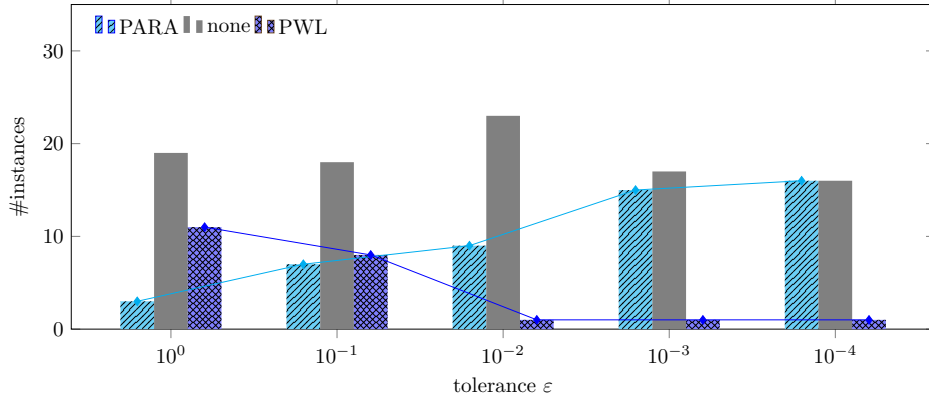


FIGURE 9. Number (#) of instances without ln solved faster by PARA or PWL per tolerance ε .

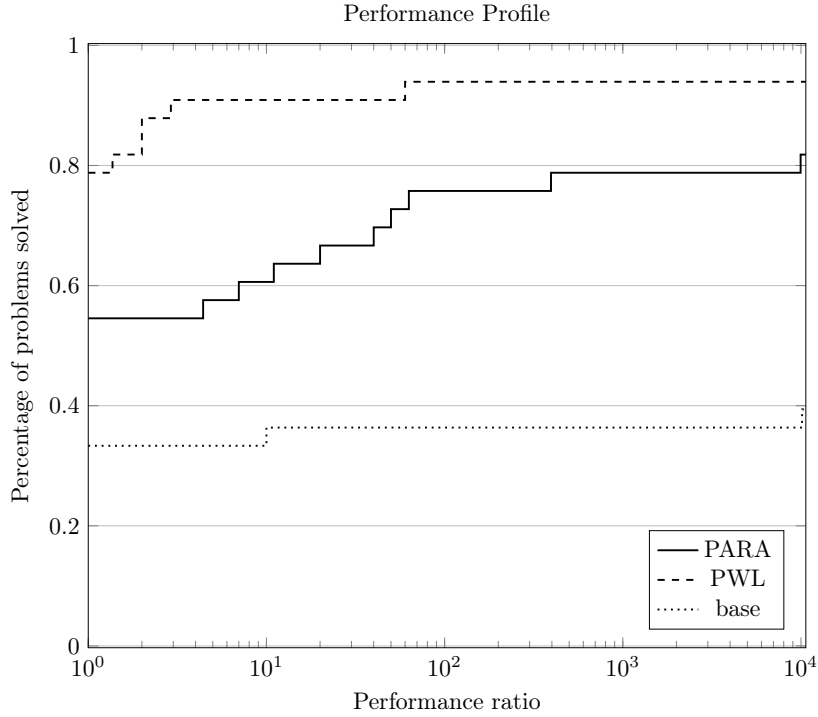


FIGURE 10. PARA and PWL for $\varepsilon = 10^0$ and base runs on instances without ln.

This makes PARA relaxations particularly advisable for usage in fields with power network optimization like AC-OPF problems [1, 7, 24].

Lastly, we'd only like to mention that the relaxation techniques were able to provide dual bounds that improve on the ones reported and achieved during base runs. We report them and give a quick overview in Table 4 in Appendix B.

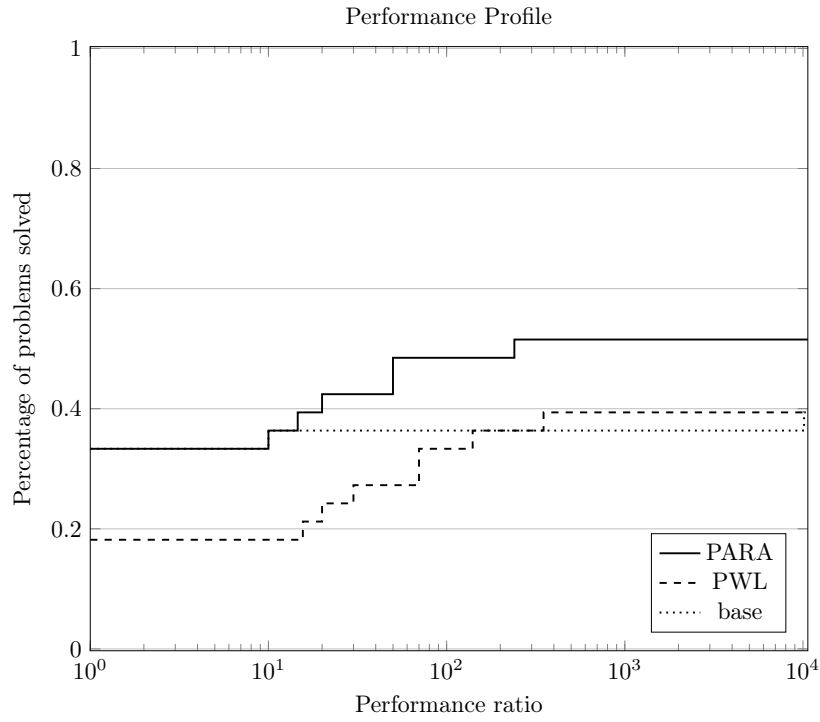


FIGURE 11. PARA and PWL for $\varepsilon = 10^{-2}$ and base runs on instances without ln.

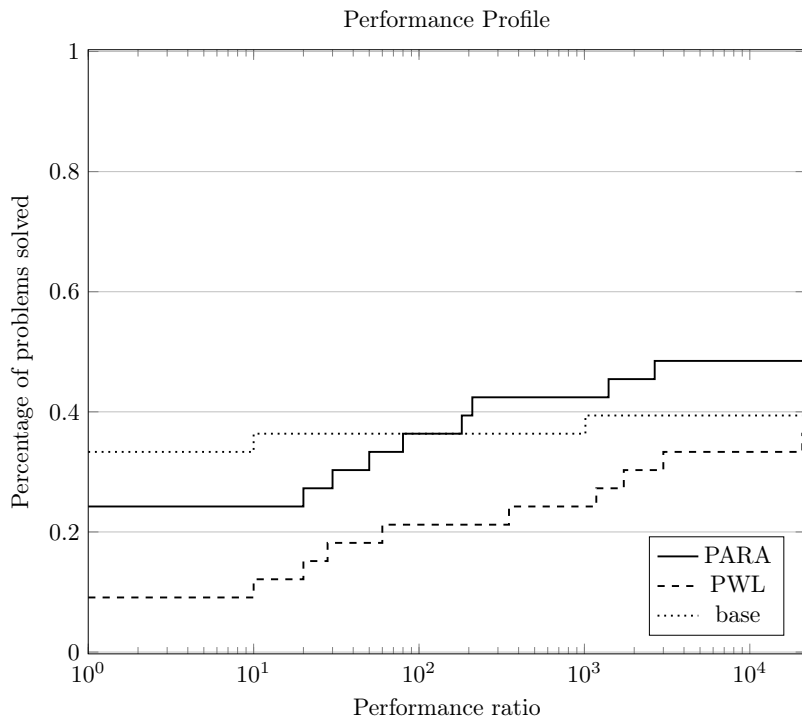


FIGURE 12. PARA and PWL for $\varepsilon = 10^{-4}$ and base runs on instances without ln.

5. CONCLUSION

We have introduced a novel method to compute PARA approximations for one-dimensional, continuously differentiable functions, which outperformed the existing method in terms of success in formerly intractable cases and mostly returned fewer parabolas. The theoretical basis was complemented with a comparison to PWL with respect to number of linear pieces/parabolas: Whereas PARA approximations for the sine function require less approximates than PWL ones throughout different interval sizes, for the natural logarithm PWL seems to require less such with increasing interval size. This is accounted to the global underestimation property causing troubles when there exists a steep slope converging asymptotically to zero.

The “clash” or comparison of PARA and PWL as MINLP relaxations was performed on a subset of the well-established MINLP Lib. Hereby, PWL relaxations seem to be particularly favorable for wider tolerances, since they require only a few binary variables and linear constraints. This favor shifts towards PARA for tighter tolerances, as the problem sizes for PWL grows too large, whereas many quadratic constraints without additional variables appears to be quite tractable. As before, there also exists a preference for trigonometric functions when using PARA, as they appear in power network optimization.

Although considering a fixed tolerance provides a valid insight for the usage of either relaxation, practical solvers iteratively refine the given relaxation until a satisfactory tolerance is reached. For PARA, this requires further theoretical developments and extended implementation effort, thus being out of reach for the present article. However, the adjustment of the presented method and a comparison with adaptive PWL relaxations appears to be a natural next step.

ACKNOWLEDGMENTS

We thank the Deutsche Forschungsgemeinschaft for their support within project A05 in the “Sonderforschungsbereich/Transregio 154 Mathematical Modelling, Simulation and Optimization using the Example of Gas Networks”, project ID 239904186. We also thank Robert Burlacu, Alexander Martin, and Kristina Rolsing for fruitful discussions about this topic and for reviewing an earlier draft.

REFERENCES

- [1] K.-M. Aigner, R. Burlacu, F. Liers, and A. Martin. “Solving AC optimal power flow with discrete decisions to global optimality.” In: *INFORMS J. Comput.* 35.2 (2023), pp. 458–474. DOI: [10.1287/ijoc.2023.1270](https://doi.org/10.1287/ijoc.2023.1270).
- [2] R. C. Baliban, J. A. Elia, R. Misener, and C. A. Floudas. “Global optimization of a MINLP process synthesis model for thermochemical based conversion of hybrid coal, biomass, and natural gas to liquid fuels.” In: *Computers & Chemical Engineering* 42 (2012), pp. 64–86.
- [3] B. Beach, R. Burlacu, A. Bärmann, L. Hager, and R. Hildebrand. “Enhancements of discretization approaches for non-convex mixed-integer quadratically constrained quadratic programming: Part I.” In: *Computational Optimization and Applications* 87.3 (2024), pp. 835–891.
- [4] B. Beach, R. Hildebrand, and J. Huchette. “Compact mixed-integer programming formulations in quadratic optimization.” In: *J. Global Optim.* 84.4 (2022), pp. 869–912. DOI: [10.1007/s10898-022-01184-6](https://doi.org/10.1007/s10898-022-01184-6).
- [5] P. Belotti, C. Kirches, S. Leyffer, J. Linderoth, J. Luedtke, and A. Mahajan. “Mixed-integer nonlinear optimization.” In: *Acta Numerica* 22 (2013), pp. 1–131. DOI: [10.1017/S0962492913000032](https://doi.org/10.1017/S0962492913000032).

- [6] P. Belotti, J. Lee, L. Liberti, F. Margot, and A. Wächter. “Branching and bounds tightening techniques for non-convex MINLP.” In: *Optimization Methods & Software* 24.4-5 (2009), pp. 597–634.
- [7] D. Bienstock, M. Escobar, C. Gentile, and L. Liberti. “Mathematical programming formulations for the alternating current optimal power flow problem.” In: *4OR* 18 (2020), pp. 249–292. DOI: [10.1007/s10288-020-00455-w](https://doi.org/10.1007/s10288-020-00455-w).
- [8] C. Bragalli, C. D’Ambrosio, J. Lee, A. Lodi, and P. Toth. “On the optimal design of water distribution networks: a practical MINLP approach.” In: *Optimization and Engineering* 13.2 (2012), pp. 219–246.
- [9] K. Braun and R. Burlacu. *Benchmarking piecewise linear reformulations for MINLPs: A computational study based on the open-source framework PWL-T-REX*. 2023. URL: <https://optimization-online.org/?p=24335>.
- [10] C. Buchheim, M. De Santis, L. Palagi, and M. Piacentini. “An exact algorithm for nonconvex quadratic integer minimization using ellipsoidal relaxations.” In: *SIAM J. Optim.* 23.3 (2013), pp. 1867–1889. DOI: [10.1137/120878495](https://doi.org/10.1137/120878495).
- [11] C. Buchheim and A. Wiegele. “Semidefinite relaxations for non-convex quadratic mixed-integer programming.” In: *Math. Program.* 141.1-2 (2013), pp. 435–452. DOI: [10.1007/s10107-012-0534-y](https://doi.org/10.1007/s10107-012-0534-y).
- [12] R. Burlacu, B. Geißler, and L. Schewe. “Solving mixed-integer nonlinear programmes using adaptively refined mixed-integer linear programmes.” In: *Optimization Methods and Software* 35.1 (2020), pp. 37–64.
- [13] M. R. Bussieck, A. S. Drud, and A. Meeraus. “MINLPLib—a collection of test models for mixed-integer nonlinear programming.” In: *INFORMS J. Comput.* 15.1 (2003), pp. 114–119. DOI: [10.1287/ijoc.15.1.114.15159](https://doi.org/10.1287/ijoc.15.1.114.15159).
- [14] J. S. Cohen. *Computer algebra and symbolic computation: elementary algorithms*. AK Peters/CRC Press, 2003.
- [15] G. D. Corporation. *General Algebraic Modeling System (GAMS)*. Version 51.3.0. Oct. 27, 2025. URL: <https://www.gams.com/>.
- [16] K. L. Croxton, B. Gendron, and T. L. Magnanti. “A comparison of mixed-integer programming models for nonconvex piecewise linear cost minimization problems.” In: *Management Science* 49.9 (2003), pp. 1268–1273.
- [17] M. Cuesta, C. D’Ambrosio, M. Durban, V. Guerrero, and R. S. Trindade. *On leveraging constrained smooth additive regression models for global optimization*. 2025. arXiv: [2510.14122](https://arxiv.org/abs/2510.14122) [math.OA]. URL: <https://arxiv.org/abs/2510.14122>.
- [18] C. D’Ambrosio, A. Frangioni, and C. Gentile. “Strengthening the Sequential Convex MINLP Technique by Perspective Reformulations.” In: *Optimization Letters* 13 (2019), pp. 673–684. DOI: [10.1007/s11590-018-1360-9](https://doi.org/10.1007/s11590-018-1360-9).
- [19] C. D’Ambrosio, J. Lee, D. Skipper, and D. Thomopulos. “Handling separable non-convexities using disjunctive cuts.” In: *Combinatorial optimization*. Vol. 12176. Lecture Notes in Comput. Sci. Springer, Cham, 2020, pp. 102–114. DOI: [10.1007/978-3-030-53262-8_9](https://doi.org/10.1007/978-3-030-53262-8_9).
- [20] C. D’Ambrosio, J. Lee, and A. Wächter. “An Algorithmic Framework for MINLP with Separable Non-Convexity.” In: *Mixed Integer Nonlinear Programming*. Ed. by J. Lee and S. Leyffer. Vol. 154. The IMA Volumes in Mathematics and its Applications. New York: Springer, 2012, pp. 315–347.
- [21] S. Elloumi, A. Lambert, B. Neveu, and G. Trombettoni. “Global solution of quadratic problems using interval methods and convex relaxations.” In: *J. Global Optim.* 91.2 (2025), pp. 331–353. DOI: [10.1007/s10898-024-01370-8](https://doi.org/10.1007/s10898-024-01370-8).
- [22] FICO. *The FICO-Xpress Optimizer*. <https://www.fico.com/fico-xpress-optimization/docs/latest/overview.html>. 2025.

- [23] R. Fourer, J. Ma, and K. Martin. “OSiL: an instance language for optimization.” In: *Comput. Optim. Appl.* 45.1 (2010), pp. 181–203. DOI: [10.1007/s10589-008-9169-6](https://doi.org/10.1007/s10589-008-9169-6).
- [24] S. Frank and S. Rebennack. “An introduction to optimal power flow: Theory, formulation, and examples.” In: *IIE Transactions* 48.12 (2016), pp. 1172–1197. DOI: [10.1080/0740817X.2016.1189626](https://doi.org/10.1080/0740817X.2016.1189626).
- [25] D. M. Gay. “Using expression graphs in optimization algorithms.” In: *Mixed integer nonlinear programming*. Vol. 154. IMA Vol. Math. Appl. Springer, New York, 2012, pp. 247–262.
- [26] A. Göß, R. Burlacu, and A. Martin. *Parabolic Approximation & Relaxation for MINLP*. 2025. arXiv: [2407.06143 \[math.OC\]](https://arxiv.org/abs/2407.06143). URL: <https://arxiv.org/abs/2407.06143>.
- [27] Gurobi Optimization, LLC. *Gurobi Optimizer Reference Manual*. 2024. URL: <https://www.gurobi.com>.
- [28] C. Hojny, M. Besançon, K. Bestuzheva, S. Borst, A. Chmiela, J. Dionísio, L. Eifler, M. Ghanam, A. Gleixner, A. Göß, A. Hoen, R. van der Hulst, D. Kamp, T. Koch, K. Kofler, J. Lentz, S. J. Maher, G. Mexi, E. Mühmer, M. E. Pfetsch, S. Pokutta, F. Serrano, Y. Shinano, M. Turner, S. Vigerske, M. Walter, D. Weninger, and L. Xu. *The SCIP Optimization Suite 10.0*. Technical Report. Optimization Online, Nov. 2025. URL: <https://optimization-online.org/2025/11/the-scip-optimization-suite-10-0/>.
- [29] J. Huchette and J. P. Vielma. “Nonconvex piecewise linear functions: Advanced formulations and simple modeling tools.” In: *Operations Research* 71.5 (2023), pp. 1835–1856.
- [30] T. Koch, B. Hiller, M. E. Pfetsch, and L. Schewe. *Evaluating gas network capacities*. SIAM, 2015.
- [31] H. M. Markowitz and A. S. Manne. “On the solution of discrete programming problems.” In: *Econometrica* 25 (1957), pp. 84–110. DOI: [10.2307/1907744](https://doi.org/10.2307/1907744).
- [32] G. P. McCormick. “Computability of global solutions to factorable nonconvex programs. I. Convex underestimating problems.” In: *Math. Programming* 10.2 (1976), pp. 147–175. DOI: [10.1007/BF01580665](https://doi.org/10.1007/BF01580665).
- [33] R. Misener and C. A. Floudas. “ANTIGONE: Algorithms for coNTinuous/Integer Global Optimization of Nonlinear Equations.” In: *J. Global Optim.* 59.2-3 (2014), pp. 503–526. DOI: [10.1007/s10898-014-0166-2](https://doi.org/10.1007/s10898-014-0166-2).
- [34] R. Misener and C. A. Floudas. “GloMIQO: global mixed-integer quadratic optimizer.” In: *J. Global Optim.* 57.1 (2013), pp. 3–50. DOI: [10.1007/s10898-012-9874-7](https://doi.org/10.1007/s10898-012-9874-7).
- [35] A. Morsi. *Solving MINLPs on Loosely-coupled Networks with Applications in Water and Gas Network Optimization: Lösungsansätze Für MINLPs Auf Schwach-gekoppelten Netzwerken Mit Anwendungen in Der Optimierung Von Wasser-und Gasnetzen*. Verlag Dr. Hut, 2013.
- [36] S. Rebennack and J. Kallrath. “Continuous piecewise linear delta-approximations for univariate functions: computing minimal breakpoint systems.” In: *Journal of Optimization Theory and Applications* 167.2 (2015), pp. 617–643.
- [37] N. V. Sahinidis. “BARON: A general purpose global optimization software package.” In: *Journal of Global Optimization* 8.2 (1996), pp. 201–205.
- [38] H. Schichl and A. Neumaier. “Interval analysis on directed acyclic graphs for global optimization.” In: *J. Global Optim.* 33.4 (2005), pp. 541–562. DOI: [10.1007/s10898-005-0937-x](https://doi.org/10.1007/s10898-005-0937-x).

- [39] A. S. Siqueira, R. G. C. da Silva, and L.-R. Santos. “Perprof-py: A python package for performance profile of mathematical optimization software.” In: *Journal of Open Research Software* 4.1 (2016), e12–e12.
- [40] Y. Song and C. T. Maravelias. “Constructing optimal piecewise quadratic approximations for enhancing deterministic global optimization.” In: *INFORMS Journal on Computing* (2025). DOI: [10.1287/ijoc.2024.0909](https://doi.org/10.1287/ijoc.2024.0909).
- [41] J. P. Vielma. “Mixed Integer Linear Programming Formulation Techniques.” In: *SIAM Review* 57.1 (2015), pp. 3–57. DOI: [10.1137/130915303](https://doi.org/10.1137/130915303).
- [42] S. Wiese. *A computational practicability study of MIQCQP reformulations*. 2021. URL: <https://docs.mosek.com/whitepapers/miqcqp.pdf>.

APPENDIX A. PROOFS FOR CORRECTNESS THEOREMS IN SECTION 3.1

In this section, we provide the detailed proofs for Theorem 3 and Theorem 4. For the sake of completeness, we restate them and provide the proof afterwards.

A.1. Proof of Theorem 3.

Theorem 3 (Correctness of Method 1). *If there exists a solution (a, b, c) fulfilling (9) and (12), Method 1 returns one or converges to it. Otherwise, it returns that there is no such solution.*

Proof. First of all, note that the results in Lemma 1 suggest that there exists a solution (a, b, c) for (9) and (12) if and only if there exist finite bounds

$$\underline{a} \geq \sup_{x \in \text{int}(\mathcal{D}_{\text{loc}})} A(x)$$

and

$$\bar{a} \leq \min \left\{ \inf_{x \in \mathcal{D} \setminus \mathcal{D}_{\text{loc}}} A(x), \inf_{x \in \text{int}(\mathcal{D}_{\text{loc}})} B(x) \right\}$$

with $\underline{a} \leq \bar{a}$. In other terms, $\underline{a} > \bar{a}$ if and only if there exists no such solution.

Assume first that there exists a solution (a, b, c) . Further, let l be the iteration index of the while-loop, i.e., the initialization sets $\bar{a}_0, \underline{a}_0 \leftarrow -\infty$, and $a_0 \leftarrow \bar{a}_0$ and every update increments l . With this notation it holds true that $\underline{a}_l \leq \underline{a}$ and $\bar{a}_l \leq \bar{a}$ for all $l \in \mathbb{N}_0$. In turn, since a_l is always chosen to be \bar{a}_l , it is $a_l \geq \underline{a}$ for all $l \in \mathbb{N}_0$ and thus the condition (9b) is always met on \mathcal{D}_{loc} .

Method 1 has two potential outcomes: Either it returns a solution in Step 6 or it executes the while-loop infinitely often. In the former case, the solution is valid for (9) by the definition of the maxima in (14), as well as satisfies (12) by construction.

If Method 1 does not return a solution, it produces a sequence of points $(x_l)_{l \in \mathbb{N}_0}$ that achieve the maximum of (14a) and (14c) and a sequence of $(a_l)_l$ from evaluating the respective term in Lemma 1 at x_l .

Note that by using the equalities (12) we can write the parabola p as parameterized in the quadratic coefficient a . Specifically, subtraction and a rearrangement of (12) gives

$$b = \frac{f(\bar{t}) - f(\underline{t})}{\bar{t} - \underline{t}} - a(\bar{t} + \underline{t}).$$

Plugging this back into either of the equalities and rearranging for c leads to

$$c = f(\underline{t}) - \varepsilon + \underline{t} \left(a\bar{t} - \frac{f(\bar{t}) - f(\underline{t})}{\bar{t} - \underline{t}} \right)$$

and

$$c = f(\bar{t}) - \varepsilon + \bar{t} \left(a\underline{t} - \frac{f(\bar{t}) - f(\underline{t})}{\bar{t} - \underline{t}} \right),$$

respectively. The parameterized version of a parabola p is then given as

$$\begin{aligned} p(x; a) &= a(x^2 - (\bar{t} + \underline{t})x + \bar{t}\underline{t}) + (x - \underline{t}) \left(\frac{f(\bar{t}) - f(\underline{t})}{\bar{t} - \underline{t}} \right) + f(\underline{t}) - \varepsilon \\ &= a(x^2 - (\bar{t} + \underline{t})x + \bar{t}\underline{t}) + (x - \bar{t}) \left(\frac{f(\bar{t}) - f(\underline{t})}{\bar{t} - \underline{t}} \right) + f(\bar{t}) - \varepsilon. \end{aligned} \tag{15}$$

The term in brackets after a can also be written as $q(x) := (\bar{t} - x)(\underline{t} - x)$. Note that q is a convex parabola symmetric to its global minimum at $(\bar{t} + \underline{t})/2$ and thus attains its maximum as \underline{x} or \bar{x} . We denote the corresponding function values as q_{min} and q_{max} . Further, see that $q(x) > 0$ for $x \in \mathcal{D} \setminus \mathcal{D}_{\text{loc}}$, whereas $q(x) < 0$ for

$x \in \text{int}(\mathcal{D}_{\text{loc}})$. Combined with the fact that a_l is non-increasing throughout the method, i.e., $a_l \leq a_{l-1}$, this representation allows to derive

$$p(x; a_l) \leq p(x; a_{l-1}), \quad \text{for } x \in \mathcal{D} \setminus \mathcal{D}_{\text{loc}}, \quad (16)$$

and

$$p(x; a_l) \geq p(x; a_{l-1}), \quad \text{for } x \in \text{int}(\mathcal{D}_{\text{loc}}). \quad (17)$$

Now, we aim to show that

- (a) for all $x \in \mathcal{D} \setminus \mathcal{D}_{\text{loc}}$, $\lim_{l \rightarrow \infty} p(x; a_l) - f(x) \leq 0$, and
- (b) for all $x \in \mathcal{D}_{\text{loc}}$, $\lim_{l \rightarrow \infty} p(x; a_l) - f(x) + \varepsilon \geq 0$.

We start with case (a). Without loss of generality, $\mathcal{D} \setminus \mathcal{D}_{\text{loc}} \neq \emptyset$, otherwise we are done. It follows that $\underline{x} < \underline{t}$ or $\bar{t} < \bar{x}$, thus $q_{\text{max}} > 0$.

We aim to prove the case by contradiction and thus assume there exists $\tilde{x} \in \mathcal{D} \setminus \mathcal{D}_{\text{loc}}$ such that

$$p(\tilde{x}; a_l) - f(\tilde{x}) > \nu, \quad \text{for all } l \in \mathbb{N}_0,$$

for a $\nu > 0$. Let x_l^1 and x_l^3 denote the optimal points for (14a) and (14c) in iteration l , respectively. Then, $a_{l+1} = \bar{a}_{l+1} = \min\{A(x_l^1), B(x_l^3)\}$ and by Lemma 1(a) it follows that $p(x_l^1; a_{l+1}) \leq f(x_l^1)$.

In turn, this implies that $(x_l^1)_{l \in \mathbb{N}_0}$ is a sequence of distinct points and, as they represent the optimal point, it is

$$p(x_l^1; a_l) - f(x_l^1) \geq p(\tilde{x}; a_l) - f(\tilde{x}) > \nu, \quad \text{for all } l \in \mathbb{N}_0.$$

Combining both statements, we have

$$\begin{aligned} \nu &< p(x_l^1; a_l) - f(x_l^1) \leq p(x_l^1; a_l) - f(x_l^1) - (p(x_l^1; a_{l+1}) - f(x_l^1)) \\ &= p(x_l^1; a_l) - p(x_l^1; a_{l+1}) = (a_l - a_{l+1})q(x_l^1) \leq (a_l - a_{l+1})q_{\text{max}}. \end{aligned}$$

A rearrangement gives $a_{l+1} < a_l - \nu/q_{\text{max}}$, which implies $a_l \rightarrow -\infty$ for $l \rightarrow \infty$, when applying induction. This is a contradiction to $-\infty < \underline{a} \leq \bar{a} \leq a_l$ for all $l \in \mathbb{N}_0$.

For case (b), we can proceed analogously. So, $\text{int}(\mathcal{D}_{\text{loc}}) \neq \emptyset$ without loss and we thus know $q_{\text{min}} < 0$. We assume there exists $\tilde{x} \in \text{int}(\mathcal{D}_{\text{loc}})$ such that

$$p(\tilde{x}; a_l) - f(\tilde{x}) + \varepsilon < -\nu, \quad \text{for all } l \in \mathbb{N}_0,$$

for a $\nu > 0$. By Lemma 1(c) and the statements from before we can follow that $p(x_l^3; a_{l+1}) \geq f(x_l^3) - \varepsilon$ for $l \in \mathbb{N}_0$. In addition, we derive

$$f(x_l^3) - p(x_l^3; a_l) - \varepsilon \geq f(\tilde{x}) - p(\tilde{x}; a_l) - \varepsilon > -\nu, \quad \text{for all } l \in \mathbb{N}_0.$$

A combination of the statements leads to

$$-\nu < p(x_l^3; a_{l+1}) - p(x_l^3; a_l) \leq (a_{l+1} - a_l)q_{\text{min}},$$

and thus $a_{l+1} < a_l - \nu/q_{\text{min}}$. This implies the same contradiction as before and we have shown case (b). In conclusion, if there exists a feasible solution (a, b, c) , Method 1 converges to it.

In the light of Lemma 1 the above results also imply that $\bar{a}_l \rightarrow \bar{a}$ for $l \rightarrow \infty$. If there exists no solution (a, b, c) , the introductory statements imply that $\underline{a} > \bar{a}$. That is, there exists some $L \in \mathbb{N}$ such that $\underline{a} > \bar{a}_l$ for all $l \geq L$ and, in turn, there exists $\tilde{x} \in \mathcal{D}_{\text{loc}}$ such that $p(\tilde{x}; \bar{a}_l) > f(\tilde{x})$.

For the update of \bar{a}_l , note that there exist x_{l-1}^1 and x_{l-1}^3 that cause it. Then, either $p(x_{l-1}^1; \bar{a}_l) = f(x_{l-1}^1)$ or $p(x_{l-1}^3; \bar{a}_l) = f(x_{l-1}^3) - \varepsilon$. In conclusion, to mitigate the violation in \tilde{x} , there needs to be a reduction in parameter \underline{a}_l in the next iteration, whereas this directly causes the respective equality to be violated again. Hence, the method has found a pair $\underline{a}_l < \bar{a}$ and exits the while-loop. \square

A.2. Proof of Theorem 4.

Theorem 4 (Correctness of Method 2). *Let $\mathcal{D} \neq \emptyset$, $f : \mathcal{D} \rightarrow \mathbb{R}$ be globally Lipschitz continuous with $L > 0$ and $\varepsilon > 0$. Then, for any interval length $\Delta > 0$ with $\Delta \leq \varepsilon/(3L)$ and $|\mathcal{D}|/\Delta \in \mathbb{N}$, one can choose \mathcal{D}_k as a partition of \mathcal{D} with $|\mathcal{D}_k| = \Delta$ and by setting $a_k = -4L/\Delta$ there exist parabolas $p_k(x) = a_k x^2 + b_k + c_k$, $k \in [|\mathcal{D}|/\Delta]$, fulfilling the properties (6) and (8).*

Proof. Consider a local interval $\mathcal{D}_k = \mathcal{D}_{\text{loc}} = [\underline{t}, \bar{t}]$ with $|\mathcal{D}_{\text{loc}}| = \Delta$. We show that there exists a particular p such that

- a) $p(x) \geq f(x) - \varepsilon$ on \mathcal{D}_{loc} ,
- b) $p(x) \leq f(x)$ on \mathcal{D}_{loc} , and
- c) $p(x) \leq f(x)$ on $\mathcal{D} \setminus \mathcal{D}_{\text{loc}}$.

For case a) we make use of Lemma 1, whereas for cases b) and c) the approach is straightforward. Throughout the following section denote the mid point of \mathcal{D}_{loc} as $\bar{t} = (\bar{t} + \underline{t})/2$.

Case a). Without loss of generality, consider $x \in \text{int}(\mathcal{D}_{\text{loc}})$. This implies $(x - \underline{t})(x - \bar{t}) < 0$.

If we can show that $a_k = -4L/\Delta \leq B(x)$, we have proven case a) by Lemma 1. We make a distinction and consider $x \in (\underline{t}, \bar{t}]$ first. Then, the distance of \bar{t} to x is at most $\Delta/2$. Formally, this is $\bar{t} - x \geq \Delta/2$ or equivalently $x - \bar{t} \leq -\Delta/2$.

By the Lipschitz continuity of f , it is

$$-L|x - y| \leq -|f(x) - f(y)| \leq f(x) - f(y) \leq |f(x) - f(y)| \leq L|x - y|,$$

for $y \in \mathcal{D}_{\text{loc}}$. Combining it with $(x - \underline{t})(x - \bar{t}) < 0$ and respecting $x - \bar{t} < 0$ we can now estimate

$$\begin{aligned} B(x) &= \frac{f(x) - f(\underline{t})}{(x - \underline{t})(x - \bar{t})} - \frac{f(\bar{t}) - f(\underline{t})}{(\bar{t} - \underline{t})(x - \bar{t})} \\ &\geq \frac{L|x - \underline{t}|}{(x - \underline{t})(x - \bar{t})} - \frac{-L|\bar{t} - \underline{t}|}{(\bar{t} - \underline{t})(x - \bar{t})} \\ &= \frac{2L}{x - \bar{t}} \geq -\frac{4L}{\Delta} = a_k, \end{aligned}$$

This was to show and concludes the first part of case a).

It remains to consider $x \in [\bar{t}, \bar{t})$. Analogously, we derive $\underline{t} - x \leq -\Delta/2$. Now, we recall that $B(x)$ has an equivalent reformulation, as stated in Remark 2, that says

$$B(x) = \frac{f(x) - f(\bar{t})}{(x - \underline{t})(x - \bar{t})} - \frac{f(\bar{t}) - f(\underline{t})}{(\bar{t} - \underline{t})(x - \underline{t})}.$$

Following the previous strategy, we get

$$\begin{aligned} B(x) &\geq \frac{L|x - \bar{t}|}{(x - \underline{t})(x - \bar{t})} - \frac{L|\bar{t} - \underline{t}|}{(\bar{t} - \underline{t})(x - \underline{t})} \\ &\geq -\frac{L}{x - \underline{t}} - \frac{L}{x - \underline{t}} \geq -\frac{4L}{\Delta} = a_k. \end{aligned}$$

Note that we have used $|x - \bar{t}| = -(x - \bar{t})$. This concludes case a).

Case b). We make the same distinction as in case a) and consider $x \in (\underline{t}, \bar{t}]$ first. Thus $x - \underline{t} \leq \Delta/2$ and $\bar{t} - x \leq \Delta$. By the Lipschitz continuity of f , we can derive

$$f(\underline{t}) - f(x) \leq |f(\underline{t}) - f(x)| \leq L|\underline{t} - x| \leq \frac{1}{2}L\Delta,$$

or equivalently $f(\underline{t}) \leq f(x) + \frac{1}{2}L\Delta$. Using the parameterized version of p as stated in (15), this gives

$$\begin{aligned} p(x; a_k) &= -\frac{4L}{\Delta}(x - \underline{t})(x - \bar{t}) + (x - \underline{t})\frac{f(\bar{t}) - f(\underline{t})}{\bar{t} - \underline{t}} + f(\underline{t}) - \varepsilon \\ &\leq (x - \underline{t})\left(L + \frac{4L}{\Delta}(\bar{t} - x)\right) + f(\underline{t}) - \varepsilon \\ &\leq \frac{1}{2}\Delta\left(L + \frac{4L}{\Delta}\Delta\right) + \frac{1}{2}L\Delta + f(x) - \varepsilon \\ &\leq \frac{5}{2}L\Delta + \frac{1}{2}L\Delta + f(x) - \varepsilon = f(x) + 3L\Delta - \varepsilon \leq f(x), \end{aligned}$$

where the last inequality follows from the assumption on Δ .

Considering $x \in [\bar{t}, \bar{t})$, we can make an analogous derivation. That is, we have $\bar{t} - x \leq \Delta/2$ and $x - \underline{t} \leq \Delta$, as well as $f(\bar{t}) \leq f(x) + \frac{1}{2}\Delta$. Combining this, we get

$$\begin{aligned} p(x; a_k) &= -\frac{4L}{\Delta}(x - \underline{t})(x - \bar{t}) + (x - \bar{t})\frac{f(\bar{t}) - f(\underline{t})}{\bar{t} - \underline{t}} + f(\bar{t}) - \varepsilon \\ &\leq (\bar{t} - x)\left(L + \frac{4L}{\Delta}(x - \underline{t})\right) + f(\bar{t}) - \varepsilon \\ &\leq \frac{1}{2}\Delta\left(L + \frac{4L}{\Delta}\Delta\right) + \frac{1}{2}L\Delta + f(x) - \varepsilon \\ &\leq \frac{5}{2}L\Delta + \frac{1}{2}L\Delta + f(x) - \varepsilon \leq f(x) + 3L\Delta - \varepsilon = f(x), \end{aligned}$$

taking the other representation of parameterized p in (15) into account. Note that the first step uses $f(\bar{t}) - f(\underline{t}) \geq -L|\bar{t} - \underline{t}|$, but the sign is turned due to $x - \bar{t} \leq 0$. This concludes case b).

Case c). First, we consider $x \in \mathcal{D}$ with $x \geq \bar{t}$. Since $p(\bar{t}) = f(\bar{t}) - \varepsilon < f(\bar{t})$, it is sufficient to show that $p' \leq f'$ for all such x . In other terms, p strictly underestimates f at \bar{t} and decreases faster than f from \bar{t} on.

Let's investigate the derivative of p at \bar{t} , which is

$$p'(\bar{t}; a_k) = -\frac{4L}{\Delta}(2\bar{t} - (\bar{t} + \underline{t})) + \frac{f(\bar{t}) - f(\underline{t})}{\bar{t} - \underline{t}} \leq -4L\frac{\bar{t} - \underline{t}}{\Delta} + L = -3L.$$

Since $a_k < 0$, p is strictly concave and thus

$$p'(x; a_k) \leq -3L < -L \leq f'(x),$$

for all $x \geq \bar{t}$.

Second, consider $x \in \mathcal{D}$ with $x \leq \underline{t}$. Analogously to above we need to show $p' \geq f'$ for all such x . Inspecting the derivative at \underline{t} gives

$$p'(\underline{t}; a_k) = -\frac{4L}{\Delta}(2\underline{t} - (\bar{t} + \underline{t})) + \frac{f(\bar{t}) - f(\underline{t})}{\bar{t} - \underline{t}} \geq 4L\frac{\bar{t} - \underline{t}}{\Delta} - L = 3L.$$

Again, due to strict concavity, we have

$$p(x; a_k) \geq 3L > L \geq f'(x),$$

for all $x \leq \underline{t}$. This concludes case c). □

TABLE 4. Dual and Gap Improvements by Relaxations

instance	sense	type	ε	time [s]	dual	rep. dual	gap [%]	rep. gap [%]
arki0017	min	PWL	10^0	limit	-9.8e2	-1.4e3	70.35	101.24
lnts100	min	PARA	10^{-4}	161	5.5e-1	5.0e-1	0.00	0.94
lnts200	min	PARA	10^{-4}	505	5.5e-1	5.0e-1	0.00	0.98
lnts400	min	PARA	10^{-3}	576	5.5e-1	4.5e-1	0.01	1.89
lnts50	min	PARA	10^{-4}	39	5.5e-1	5.1e-1	0.00	0.87
polygon100	min	PARA	10^{-3}	limit	-3.1e0	-2.8e1	29.78	352.32
polygon25	min	PARA	10^{-3}	limit	-2.2e0	-4.3e0	17.89	44.80
polygon50	min	PARA	10^{-4}	limit	-3.0e0	-1.1e1	28.47	133.76
polygon75	min	PARA	10^{-4}	limit	-3.1e0	-1.9e1	29.17	234.13
powerflow0039p	min	PARA	10^{-4}	limit	4.0e2	4.0e2	9.90	9.90
powerflow0300p	min	PARA	10^{-3}	limit	1.2e4	0	-	-
procurement1large	max	PWL	10^{-2}	limit	7.1e3	1.8e4	28.66	36.97
procurement1mot	max	PWL	10^{-1}	limit	4.6e2	1.4e3	25.74	36.89

APPENDIX B. DUAL GAP IMPROVEMENTS

As mentioned in Section 4, there exist instances for which one relaxation method resulted in improved dual bounds. We compare to the dual bounds achieved during the base run and the ones reported on the MINLPLib [13] webpage.

In Table 4 we list all instances, where at least one improvement was detected and give the respective relaxation type and tolerance. If the same type has achieved the same dual bound for several tolerances ε , we report the result for its largest value. The column “sense” reports on the objective sense in order to classify the dual bounds correctly. The gaps are computed with respect to the reported primal value on the webpage and – for the relaxations – the dual value achieved when solving a relaxation. The term “rep.” stands for “reported” and refers to the value from the reference value from the webpage.

We limit our interpretation to the “lnts” and the “polygon” instances, as they show the most significant improvements. For all those, PARA was able to construct relaxation that lead to dual bounds which can reduce the original gap to nearly zero or by a factor of up to 10, respectively. Once again, this strengthens our observation that PARA seems to be quite efficient when tackling (co)sine constraint functions, since all those are nonlinear programs with quite an extensive number of such constraints.